AD_____

Award Number: DAMD17-98-1-8523

TITLE: Chemotherapeutic and Immunotherapeutic Effects of 15-deoxy-Δ12, 14-prostaglandin J2 on Prostate Cancer

PRINCIPAL INVESTIGATOR: Charles Young, Ph.D.

CONTRACTING ORGANIZATION: Mayo Foundation
Rochester, Minnesota 55905

REPORT DATE: March 2001

TYPE OF REPORT: Final, Phase I

PREPARED FOR: U.S. Army Medical Research and Materiel Command
Fort Detrick, Maryland 21702-5012

REPORT DOCUMENTATION PAGE

Form Approved
OMB No. 074-0188

1. AGENCY USE ONLY (Leave blank)	2. REPORT DATE	3. REPORT TYPE AND DATES COVERED
	October ~~2000~~ March 2001	Final, Phase I (1 Sep 98 - 28 Feb 01)

4. TITLE AND SUBTITLE
Chemotherapeutic and Immunotherapeutic Effects of 15-deoxy-Δ12, 14-prostaglandin J2 on Prostate Cancer

5. FUNDING-NUMBERS
DAMD17-98-1-8523

6. AUTHOR(S)
Charles Young, Ph.D.

7. PERFORMING ORGANIZATION NAME(S) AND ADDRESS(ES)
Mayo Foundation
Rochester, Minnesota 55905

E-Mail: youngc@mayo.edu

8. PERFORMING ORGANIZATION REPORT NUMBER

9. SPONSORING / MONITORING AGENCY NAME(S) AND ADDRESS(ES)
U.S. Army Medical Research and Materiel Command
Fort Detrick, Maryland 21702-5012

10. SPONSORING / MONITORING AGENCY REPORT NUMBER

11. SUPPLEMENTARY NOTES

12a. DISTRIBUTION / AVAILABILITY STATEMENT
Approved for Public Release; Distribution Unlimited

12b. DISTRIBUTION CODE

13. ABSTRACT *(Maximum 200 Words)*

It has been suggested that compositions of essential fatty acids (EFAs) in diets consumed by humans can largely affect the incident rates of many cancers including prostate cancer. In fact, ω-3 polyunsaturated essential fatty acids (PUFAs) such as docosahexaenoic acid (DHA) and eicosapentaenoic acid (EPA) and one of their terminal metabolites, 15-deoxy-Δ12,14-prostaglandin J2 (15d-PGJ2) may be involved in cell growth and differentiation. The peroxisome proliferator activated receptors (PPARs) as transcription factors are the mediators for some of these hormone-like lipids. Our aims were to determine the growth responses of human prostate cells to 15d-PGJ2 and related lipids and the role of PPARγ. Additional study was to investigate the effects of DHA and EPA on androgen receptor mediated action in prostate cancer . We completed these aims. It was found that the expression and functions of PPARγ were activated by 15d-PGJ2 and DHA. PPARγ was also detected by western analysis in human prostate cancerous tissues. Moreover, in contrast to other studies with non-prostate cells, we showed that both androgen responsive and -refractory prostate cells are all induced by 15d-PGJ2 and PUFAs to undergo, instead of differentiation into adipocyte-like cells, S-phase cell cycle arrest and non-apoptotic programmed cell death. Interestingly . we discovered that DHA, 15d-PGJ2 and/or EPA can interfere with androgen receptor's function in human prostate cancer cells. Further studies seem to indicate that these PUFAs can activate an inhibitory cross-talking component, AP-1 protein, that interacted with and inhibited androgen receptor's function. Our studies provide a strong basis for the use of these PUFAs as intervening means to prevent or treat prostate cancer.

14. SUBJECT TERMS Prostate Cancer	15. NUMBER OF PAGES 28
	16. PRICE CODE

17. SECURITY CLASSIFICATION OF REPORT	18. SECURITY CLASSIFICATION OF THIS PAGE	19. SECURITY CLASSIFICATION OF ABSTRACT	20. LIMITATION OF ABSTRACT
Unclassified	Unclassified	Unclassified	Unlimited

Table of Contents

Proposal Title: Molecular mechanisms of essential fatty acids and metabolites in regulation of prostate cancer cell growth. **PI: Charles Y. F. Young, Ph. D.**

Introduction

It has been suggested (1-3) that compositions of essential fatty acids (EFAs) in diets consumed by humans can largely affect the incident rates of many cancers including prostate cancer. Whether it is a negative or positive association with the disease may depend on the types and quantity of fatty acids in the diet consumed (1-4). In fact, ω-3 polyunsaturated essential fatty acids (PUFAs) such as docosahexaenoic acid (DHA) and eicosapentaenoic acid (EPA) and one of their terminal metabolites, 15-deoxy-Δ12,14-prostaglandin J2 (15d-PGJ2) may be involved in cell growth and differentiation (5-8). The peroxisome proliferator activated receptors (PPARs) as transcription factors are the mediators for some of these hormone-like lipids (9). We hypothesize that PPARγ is the mediator for 15-deoxy-$\Delta^{12,14}$-prostaglandin J2 (15d-PGJ2), a terminal metabolite of prostaglandin J2 series, in regulation of cell growth negatively and gene expression in normal and cancerous prostates. Thus, 15d-PGJ2/PPARγ could be an intervening target for prostate cancer. Our aims were to determine the growth responses of human prostate cells to 15d-PGJ2 and related lipids and the role of PPARγ. It was found in our studies that the expression and functions of PPARγ were activated by 15d-PGJ2 and DHA. PPARγ was also detected by western analysis in human prostate cancerous tissues. Moreover, in contrast to other studies with non-prostate cells, we showed that both androgen responsive and -refractory prostate cells are all induced by 15d-PGJ2 and PUFAs to undergo, instead of differentiation into adipocyte-like cells, S-phase cell cycle arrest and non-apoptotic programmed cell death. Interestingly . we discovered that DHA and/or EPA can interfere with androgen receptor's function in human prostate cancer cells. Our studies provide a strong basis for the use of these PUFAs as intervening means to prevent or treat prostate cancer.

Report body

Statement of Work (Original Proposal):

1. Determine the growth responses of human prostate cells to 15-deoxy-Δ12-prostaglandin J2 (15d-PGJ2) and to combination of all-trans retinoic acid, 9-cis retinoic acid or vitamin D3 with 15d-PGJ2.
a.Measure growth responses of three human prostate cancer cell lines to
a number of fatty acids and prostanoids including 15d-PGJ2 and determine their relative inhibition potency (months 1-4).
b.Measure growth responses of the prostate cell lines to a combination of all-trans retinoic acid, 9-cis retinoic acid or vitamin D3 with 15d-Δ12-PGJ2 (months 5-8)
c.Using a number of assays to determine apoptosis in the prostate cells by treatment of 15d-PGJ2 (months 9-12)

2. Demonstrate the expression of PPAR proteins in prostate cells
a. Generate monospecific polyclonal antibodies for PPAR α and β (months 1-8)
b. Using weatern blot analysis to study the expression of PPARs in prostate cell lines (months 1-2 for PPAR; months 9-12)
c. Using western blot analysis and immunohistochemical staining to detect the expression of PPARs in human prostate tissues (months 3-6 for PPARγ; months 13-18)
d. Using transfection and gel band-shift assays (with PPAR specific antibodies) to demonstrate the functions of PPARs in the human prostate cell lines (months 13-18).

3. Determine the role of peroxisome proliferator activated receptor γ(PPARγ) in 15d-Δ12-PGJ2 mediated growth inhibition in prostate cancer cells
a. To make suitable LNCaP cell subline expressing tetracyclin binding protein (TBP) (work has been done).

b. To use the above LNCaP cell subline expressing TBP to construct a second subline for expressing antisense mRNAs for PPARs (months 13-18).
c. To determine whether the expression of PPAR proteins are reduced in the cell lines generated in 3.b.(months 16-18)
d. To test the growth response of the cell line generated in 3. b. to 15d-PGJ2 (months 17-24).

Research Accomplishments :
Basically, we have completed most of the three specific aims, resulting in two abstract presentations, two publication and one manuscript submission. Our observation in one of these publications (Ref#5:Cell Growth & Diff.11:49,2000) addressed most of the questions in these three aims. However, because of new findings during the course of this project, we re-directed the goals of Specific Aim 3 in which the inhibitory effects of 15d-PGJ2, docosahexaenoic acid (DHA) and eicosapentaenoic acid (EPA) on androgen regulated growth response and -gene expression were examined (this redirection in Specific Aim 3 was requested in the 1999 progress report and approved). Research findings are summarized below:

a. we demonstrated that 15d-PGJ2 as a naturally occurring ligand for peroxisome proliferator activated receptor γ (PPARγ) caused S-phase cell arrest and non-apoptotic programmed cell death but not cell differentiation of prostate cancer cells (5, also see the Appendix). The cell death and S-phase cell arrest induced by 15d-PGJ2 are not mediated via tumor suppresor p53 and cyclin dependent kinase inhibitor p21 dependent pathways. This might lead to a new avenue to elucidate novel mechanisms by which 15d-PGJ2 induce prostatic cell death. Also, it has been shown that 15d-PGJ2 is a potent anti-angiogenesis agent (6, 10, 11). Together, these studies seem to indicate that 15d-PGJ2 may be used as an intervening agent for prostate cancer.

b. It has been suggested that consuming high quantities of DHA and FPA in fish and olive oils may help reduce prostate cancer risk (2-5), however, the mechnism for that was not known.

We examined the effects of DHA and EPA on androgen-regulated expression of a well-known androgen regulated gene, PSA (12). The normalized data in figure 1A showed the dramatic decrease in androgen stimulated PSA secretion by DHA. Figure 1B with EPA treatment demonstrates a similar pattern as figure 1A except that EPA treatment required higher EPA concentrations for significant inhibition. Similar results were seen for another androgen regulated protein, hK2 (data not shown).

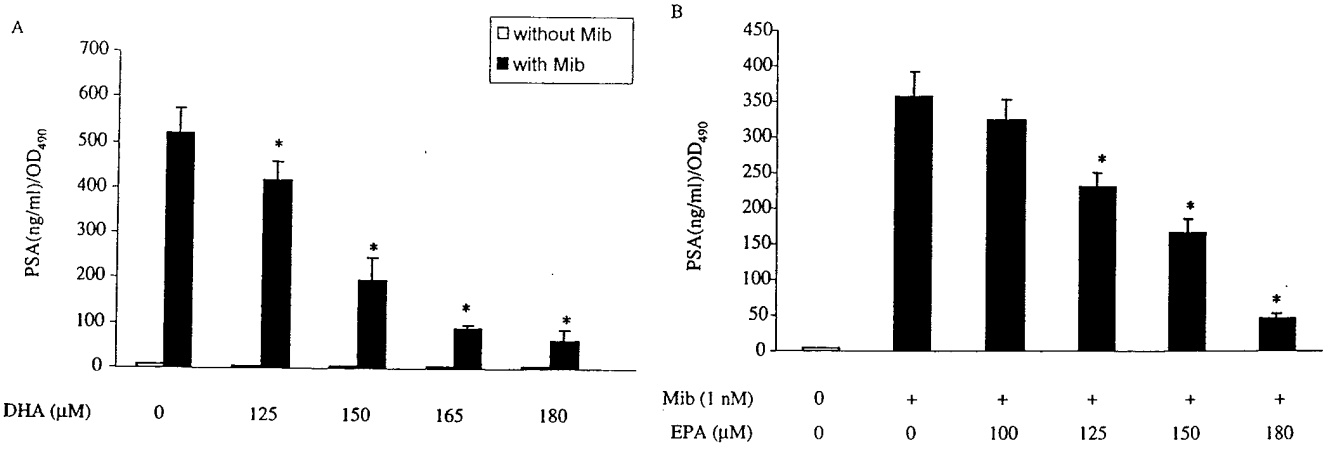

Figure 1 ***The androgen induced expression of PSA protein is affected by DHA or EPA in LNCaP Cells*** **Total PSA quantification was performed on the spent media from cells treated with DHA (A) or EPA (B). These protein levels were normalized to cell density . * depicts significant inhibition compared to the no treatment controls.**

Northern analysis was performed to see if different androgen regulated genes are affected by DHA and EPA treatment. The androgen responsive genes NKX 3.1 (13), ornithine decarboxylase (ODC) (14), the

immunophilin fkbp 51, Drg-1 (15) and PSA were all tested to ascertain the effect of the omega 3 fatty acids. Figure 2 shows that all mRNA probed were up-regulated by androgens and that the treatment with DHA greatly inhibited the induced response.

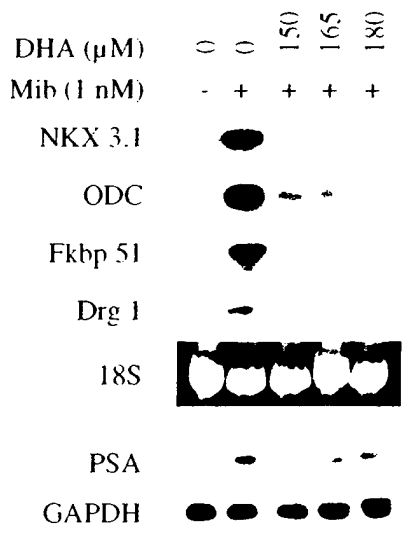

Figure 2. ***Effects of DHA on the androgen induced expression of androgen regulated genes*** **Northern blot analysis of the PSA, ODC, NKX 3.1, fkbp 51, Drg-1 and GAPDH mRNAs in LNCaP cells treated with DHA and Mib for 24 hours. The 18S ribosome RNA and GAPDH are shown as loading controls.**

Given that all the androgen inducible genes tested were inhibited at the mRNA level, the next step was to determine if DHA and EPA had any effect on the AR mediated transactivation of androgen regulated genes.

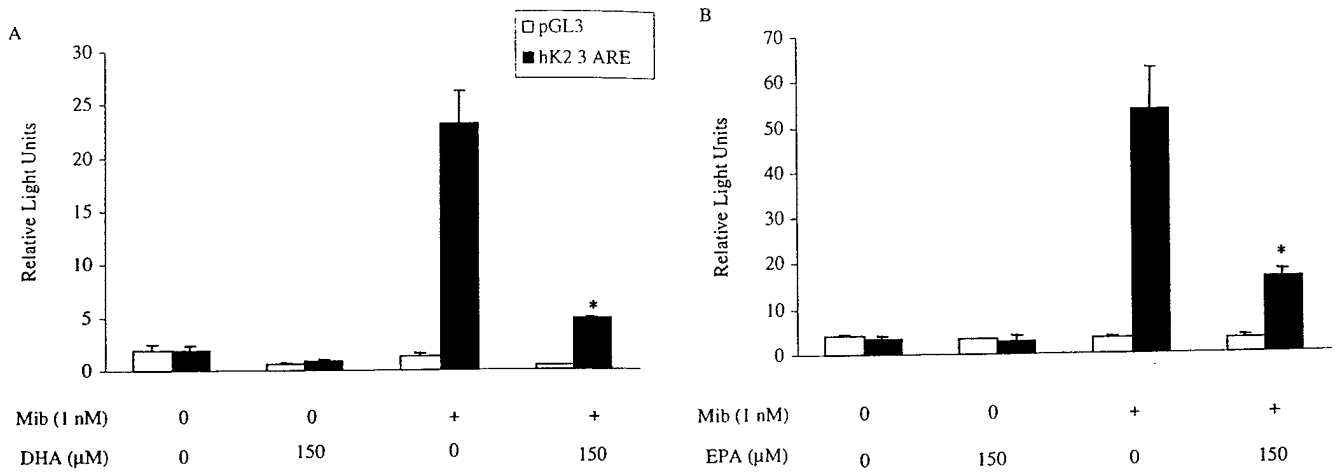

Figure 3. ***Effects of DHA and EPA on the androgen receptor mediated transcription of a heterologous reporter gene*** **A transient transfection in LNCaP cells with a PGL3 SV40 or pGL3 SV40-3 ARE was performed. After 24 hours, cells were treated with DHA (A) or EPA (B) in the presence or absence of Mib. Cell extracts were prepared for luciferase and β-galactosidase assays. Luciferase activities were normalized by ß-gal activities and presented as relative light units/mU ß-gal. The transfection was repeated three times with standard deviation bars shown. * depicts significant inhibition compared to the no treatment controls.**

Therefore, a construct containing three copies of an androgen responsive element in front of a luciferase reporter gene and an empty vector were transfected into LNCaP cells with or without Mib for 24 hours to test whether DHA or EPA can directly affect AR mediated transcriptional activity. Figure 3 shows the activity of the cells treated with or without Mib. In the Mib treated cells, the ARE gives a strong androgenic induction of luciferase activity. However, DHA and EPA treatments inhibit this androgenic response ($p < 0.05$). This assay strongly suggests that these lipids can affect the transcriptional function of AR.

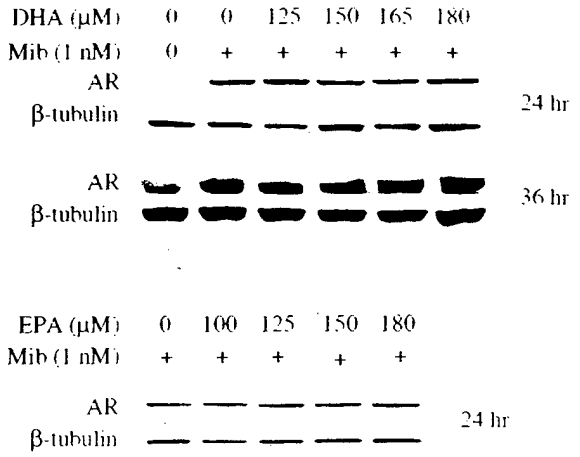

Figure 4. ***Effects of DHA and EPA on the expression of the androgen receptor protein.*** **A western blot analysis of the androgen receptor in LNCaP cells treated with varying amounts of DHA or EPA for indicated times was performed. β-tubulin was used as an internal control. The cells were treated with or without Mib for 24 hours then cell extracts were prepared for luciferase assays and the total protein was measured. The open bars represent no Mib treatment and the closed bars denote Mib treatment. The results are shown as light units/mg protein. The experiment was performed in triplicate and standard deviation bars shown.**

Furthermore, western blot analysis for AR protein was performed to determine whether the lipids have an effect on the expression of AR protein. As shown in figure 4, AR protein levels were increased by androgens which could not be changed by DHA treatments for 24 or 36 hours. Similarly EPA did not alter AR expression. Although the molecular mechanism by which these lipids modulate androgen action in prostate cells requires further elucidation, the above studies (manuscript in preparation) provide a novel finding to explain how and why these lipids can reduce prostate cancer risk.

c. We showed that 15d-PGJ2 can induce overexpression of Hsp 70 in human and mouse prostate cancer cells. Recent studies (16) suggested that non-apoptotic cell death together with overexpression of Hsp in cancer cells can enhance anti-tumor immunity. We examined if 15d-PGJ2 induced Hsp70 could generate anti-prostate cancer immunity in a mouse prostate cancer model. We demonstrated that 15d-PGJ2 induced Hsp 70 in mouse TRAMP C2 cells (purified by ADP affinity column plus Mono-Q ionic exchanger) can induce T cell immunity against the prostate cancer cells by *in vitro* cytotoxic T cell assay and *in vivo* studies (17; please also see the manuscript in Appendix). Although this work was not planned in the original proposal, it is certainly the research product from the observations of this proposed project. The progression of this study will, in fact, be supported by the Phase II proposal of this grant.

Key Research Accomplishments

1. The study provides molecular basis by which 15d-PGJ2 as a naturally occurring ligand for peroxisome proliferator activated receptor γ (PPARγ) caused non-apoptotic programmed cell death of prostate cancer cells.

2. This study provides novel molecular basis to explain how some of omega 3 fatty acids can reduce prostate cancer risk.

3. The above studies seem to indicate that 15d-PGJ2 may be potentially used as an agent for both chemotherapeutic and immunotherapeutic purposes for prostate cancer.

Reportable Outcomes

1.Chung BH, Mitchell SH, Young CYF. (2000) Effects of fish oil (docosahexaenoic acid and eicosahexaenoic acid) on androgen mediated growth response and gene expression in LNCaP prostate cancer cells. (submitted)

2. Donkena. K. V,, M. E. Grossmann, E. Celis and C. Y.F. Young, Tumor prevention and anti-tumor immunity with heat shock protein 70 induced by 15-deoxy _ ^{12,14} prostaglandin J_2 in transgenic adenocarcinoma of the mouse prostate cells. Cancer Research 60:4714-4718, 2000.

3. Donkena KV, Butler R. Mitchell SH, Young, C.Y.F, Antiproliferative activity of 15-deoxy-_ ^{12,14}-prostaglandin J_2 in prostate cancer cells is associated with activation of PPAR gamma and induction of HSP-70 expression. AACR 91st Annual Metting, April 1-5, 2000, San Francicso,CA

4. R. Butler, S. H. Mitchell, D. J. Tindall, and C, Y. F. Young, Non-apoptotic cell death associated with S-phase arrest of prostate cancer cells via the PPAR-γ ligand, 15-deoxy-$\Delta^{12,14}$-prostaglandin J_2. Cell Growth and Differentiation. 11:49-61, 2000.

5. Butler, R. and C. Y.-F. Young, 15-deoxy-$\Delta^{12,14}$-prostaglandin J_2 induces apoptosis in human prostate cancer cell lines. Keystone Symposia: Breast and Prostate Cancer, 1998 Abstract No. 204.

Involvement of Laboratory Personnel

Charles Young, Ph. D. , P.I.
Rachel Butler, Ph. D., Research Fellow
K. Vanaja Donkena, Ph. D. Research Fellow
Byung-Ha Chung, M. D., Ph. D. Research Fellow
Susan H. Mitchell, B. S., Technician

Conclusions

(A) Previous studies demonstrated that 15d-PGJ2 as a naturally occurring ligand for PPAR γ, and its synthetic analogues can induce cell differentiation of non-prostate cancer cells (7, 8). Our study (5) has demonstrated that 15d-PGJ2 causes S-phase cell arrest and non-apoptotic programmed cell death of prostate cancer cells. The cell death induced by 15d-PGJ2 are not mediated via tumor suppresor p53 and cyclin dependent kinase inhibitor p21 dependent pathways. This study seems to indicate that 15d-PGJ2/PPARγ can be a new intervening target for prostate cancer.

(B) Moreover, preliminary studies showed that the expression of several androgen regulated genes can be inhibited by EPA and DHA, suggesting that these PUFAs may interfere with androgen action in prostate cells. Androgens play an important role in development and progression of prostate cancer. Thus these dietary PUFAs and derivitives may reduce prostate cancer risk.

(C) We found that 15d-PGJ2 can induce overexpression of HSP70 in all prostate cancer cell lines tested. We also demonstrated that ADP affinity purified Hsp70 from 15d-PGJ2 treated prostate cells exhibits high potency of induction of anti-prostate cancer immunity, whereas Hsp 70 from non-prostatic cancer cells shows no anti-prostate cancer immunity effect (17). This study strongly suggests that 15d-PGJ2 induced cell death and overexpression of Hsp might enhance tumor immunity against prostate cancer.

References:

1. Giovannucci, E., Rimm E.B., Colditz G.A., Stampfer M.J., Ascherio A., Chute C.C., and Willett W.C. A prospective study of dietary fat and risk of prostate cancer. *J. Natl. Cancer Inst.* 85:1571-1579, 1993

2. Pienta K.J., and Esper P.S. Is dietary fat a risk factor for prostate cancer? J. Natl. Cancer Inst. 85:1538-1540, 1993.

3. Rose, D.P., and. Connolly J.M. Dietary fat, fatty acids and prostate cancer. Lipids. 27:798-803, 1992.

4. Pandalai, F.K., Pilat M.J., Yamazaki K., Naik H., and Pienta K.J. The effects of omega-3 and omega-6 fatty acids on in vitro prostate cancer growth. *Anticancer Res.* 16:815-820, 1996

5. Butler R. Mitchell SH, Tindall, DJ. and Young, CYF, Non-apoptotic cell death associated with S-phase arrest of prostate cancer cells via the PPAR-γ ligand, 15-deoxy-$\Delta^{12,14}$-prostaglandin J_2. Cell Growth and Differentiation. 11:49-61, 2000.

6. Rose DP. Connolly JM. Antiangiogenicity of docosahexaenoic acid and its role in the suppression of breast cancer cell growth in nude mice. International Journal of Oncology. 15(5):1011-1015, 1999.

7. Mueller, E., Sarraf P., Tontonoz P., Evans R.M., Martin K.J., Zhang M., Fletcher C., Singer S., and Spiegelman B.M. Terminal differentiation of human breast cancer through PPARg. Mol. Cell. 1:465-470, 1998

8. Tontonoz, P., Singer S., Forman B.M., Sarraf P., Fletcher J.A., Fletcher C.D., Brun R.P., Mueller E., Altiok S., Oppenheim H., Evans R.M., and Spiegelman B.M. Terminal differentiation of human liposarcoma cells induced by ligands for peroxisome proliferator-activated receptor gamma and the retinoid X receptor. Proc. Natl. Acad. Sci. USA. 94:237-241, 1997.

9. Forman B. M., Tontonoz P., Chen J., Grun R. P., Spiegelman B. M., and Evans R. M. 15-deoxy-$\Delta^{12,14}$-prostaglandin J_2 is a ligand for the adipocyte determination factor PPAR gamma. *Cell* 83:803-812, 1995.

10. Xin XH. Yang SY. Kowalski J. Gerritsen ME. Peroxisome proliferator-activated receptor gamma ligands are potent inhibitors of angiogenesis in vitro and in vivo. Journal of Biological Chemistry. 274(13):9116-9121, 1999.

11. Bishop-Bailey D. Hla T. Endothelial cell apoptosis induced by the peroxisome proliferator-activated receptor (PPAR) ligand 15-deoxy-Delta(12,14)-prostaglandin J(2) . Journal of Biological Chemistry. 274(24):17042-17048, 1999.

12. Zhu, W. Young, CYF. Transcriptional regulation of the prostate-specific antigen gene by thyroid hormone 3,5.3'-L-triiodothyronine. J. of Andrology 22:136-141, 2001

13. Xu LL., Srikantan V., Sesterhenn I.A., Augustus M., Dean R., Moul J.W., Carter K.C. and Srivastava S. Expression profile of an androgen regulated prostate specific homeobox gene NKX3.1 in primary prostate cancer. Journal of Urology. 163:972-9, 2000

14. Bai G., Kasper S., Matusik R.J., Rennie P.S., Moshier J.A. and Krongrad A. (1998) Androgen regulation of the human ornithine decarboxylase promoter in prostate cancer cells. Journal of Andrology. 13:127-135, 1998

15. Ulrix W., Swinnen J.V., Heyns W. and Verhoeven G. The differentiation related gene 1, Drg1, is markedly upregulated by androgens in LNCaP prostatic andenocarcinoma cells. FEBS Letters 455:23-26, 1999

16. Alan Melcher, Stephen Todryk, Nicola Harwick, Martin Ford, Michael Jacobson & Richard G. Vile. Tumor immunigenicity is determined by the mechanism of cell death via induction of heat shock protein expression. Nature Medicine., 4: 581-587, 1998.

17. Donkena. K. V, Grossmann, M. E., Celis E. and Young, C. Y.F. Tumor prevention and anti-tumor immunity with heat shock protein 70 induced by 15-deoxy $\Delta^{12,14}$ prostaglandin J_2 in transgenic adenocarcinoma of the mouse prostate cells. Cancer Research 60:4714-4718, 2000.

Appendix

Proposal Title: Molecular mechanisms of essential fatty acids and metabolites in regulation of prostate cancer cell growth. **PI: Charles Y. F. Young, Ph. D.**

Two manuscripts

Nonapoptotic Cell Death Associated with S-Phase Arrest of Prostate Cancer Cells via the Peroxisome Proliferator-activated Receptor γ Ligand, 15-Deoxy-$\Delta^{12,14}$-prostaglandin J_2[1]

Rachel Butler,[2] Susan H. Mitchell, Donald J. Tindall, and Charles Y. F. Young[3]

Departments of Urology [R. B., S. H. M., D. J. T., C. Y. F. Y.] and Biochemistry [D. J. T., C. Y. F. Y.] and Molecular Biology, Mayo Clinic/Foundation, Rochester, Minnesota 55905

Abstract

15-Deoxy-$\Delta^{12,14}$-prostaglandin J_2 (15d-PGJ_2) is a highly specific activator of the peroxisome proliferator-activated receptor γ (PPAR-γ). We investigated the effect of 15d-PGJ_2 on three human prostate cancer cell lines, LNCaP, DU145, and PC-3. Western blotting demonstrated that PPAR-γ1 is expressed predominantly in untreated prostate cancer cells. Treatment with 15d-PGJ_2 caused an increase in the expression of PPAR-γ2, whereas PPAR-γ1 remained at basal levels. PPARs α and β were not detected in these cells. Lack of lipid accumulation, increase in CCAAT/enhancer binding proteins (C/EBPs), or expression of aP2 mRNA indicated that adipocytic differentiation is not induced in these cells by 15d-PGJ_2. 15d-PGJ_2 and other PPAR-γ activators induced cell death in all three cell lines at concentrations as low as 2.5 μM (similar to the K_d of PPAR-γ for this ligand), coinciding with an accumulation of cells in the S-phase of the cell cycle. Activators for PPAR-α and β did not induce cell death. Staining with trypan blue and propidium iodide suggested that, although the plasma membrane appears intact by electron microscopy, disturbances are evident as early as 2 h after treatment. Mitochondrial transmembrane potentials are significantly reduced by 15d-PGJ_2 treatment. In addition, treatment with 15d-PGJ_2 resulted in cytoplasmic changes, which are indicative of type 2 (autophagic), nonapoptotic programmed cell death.

Introduction

Prostate cancer is the most common cancer in American men and the second leading cause of male cancer death (1–3). There is much experimental and epidemiological evidence to suggest that dietary fat can influence the incidence rate of prostate cancer. Essential fatty acids have been implicated in the development and progression of advanced prostate cancer (4–8). In recent years, different series of prostaglandins, the products of arachidonic fatty acid metabolism, have been shown to have either positive or negative effects on cancer cell growth (9, 10). Diets rich in fish and olive oils, containing ω-3 fatty acids, appear to be linked to a lower incidence of prostate cancer compared with the high incidence in the Western world, where the diets include a high intake of corn oil, which contains ω-6 fatty acids.

Many unsaturated, long chain fatty acids and their metabolites, including prostanoids and synthetic analogues, have been demonstrated to act as ligands/hormones via the PPAR[4]. PPAR is a member of the steroid hormone receptor superfamily involved in the ligand-inducible regulation of lipid metabolism (11–14). PPAR, retinoic acid, vitamin D, and thyroid hormone receptors belong to type II nuclear receptors (15, 16). There are three types of PPARs: PPAR-α, PPAR-β (or NUC-1 and PPAR-δ), and PPAR-γ. In addition, two isoforms of PPAR-γ, PPAR-γ1 and PPAR-γ2, are expressed in human tissues as a result of alternate transcription start sites and alternative splicing (17). These two isoforms differ only in their NH_2 termini in that PPAR-γ2 has an additional 30 amino acids (18–20). The expression of the two isoforms is differentially regulated in a tissue-specific manner. PPAR-γ2 is abundant in adipocytes and is thought to be relatively specific for this tissue (18, 21, 22). PPAR-γ1 is also highly expressed in adipocytes; however, lower levels of expression have been detected in a number of other tissues, including muscle and liver (21–23). All PPAR isoforms require heterodimerization with the retinoid X receptor for optimal DNA binding and transcriptional activity (15, 16, 23).

Received 5/28/99; revised 12/8/99; accepted 12/8/99.
The costs of publication of this article were defrayed in part by the payment of page charges. This article must therefore be hereby marked *advertisement* in accordance with 18 U.S.C. Section 1734 solely to indicate this fact.
[1] R. B., S. H. M., and C. Y-F. Y. are supported by NIH Grants DK41995 and CA70892 and by Department of Defense Grant DMAD 17-98-107-523. D. J. T. is supported by a National Cancer Institute grant to the Mayo Comprehensive Cancer Center and a grant from the T. J. Martell Foundation.
[2] Present address: Department of Clinical Neurosciences, Institute of Psychiatry, De Crespigny Park, Denmark Hill, London SE5 8AF, United Kingdom.
[3] To whom requests for reprints should be addressed, at Department of Urology, 17 Guggenheim, Mayo Clinic, 200 First Street SW, Rochester, MN 55905. Phone: (507) 284-8336; Fax: (507) 284-2384; E-mail: youngc@mayo.edu.

[4] The abbreviations used are: PPAR, peroxisome proliferator-activated receptor; 15d-PGJ_2, 15-deoxy-$\Delta^{12,14}$-prostaglandin J_2; ETYA, 5,8,11,14-eicosatetraenoic acid; EPA, eicosapentaenoic acid; DHA, docosahexaenoic acid; MTS, 3-(4,5-dimethylthiazol-2-yl)-5-(carboxymethoxyphenyl)-2(4-sulophenyl)-2H-tetrazolium; FACS, fluorescence-activated cell sorter; C/EBP, CCAAT/enhancer binding proteins; PI, propidium iodide; PARP, poly(ADP-ribose) polymerase; JC-1, 5,5′,6,6′-tetrachloro-1,1′,3,3′-tetraethylbenzimidoazolcarbocyanine iodide; PSA, prostate-specific antigen.

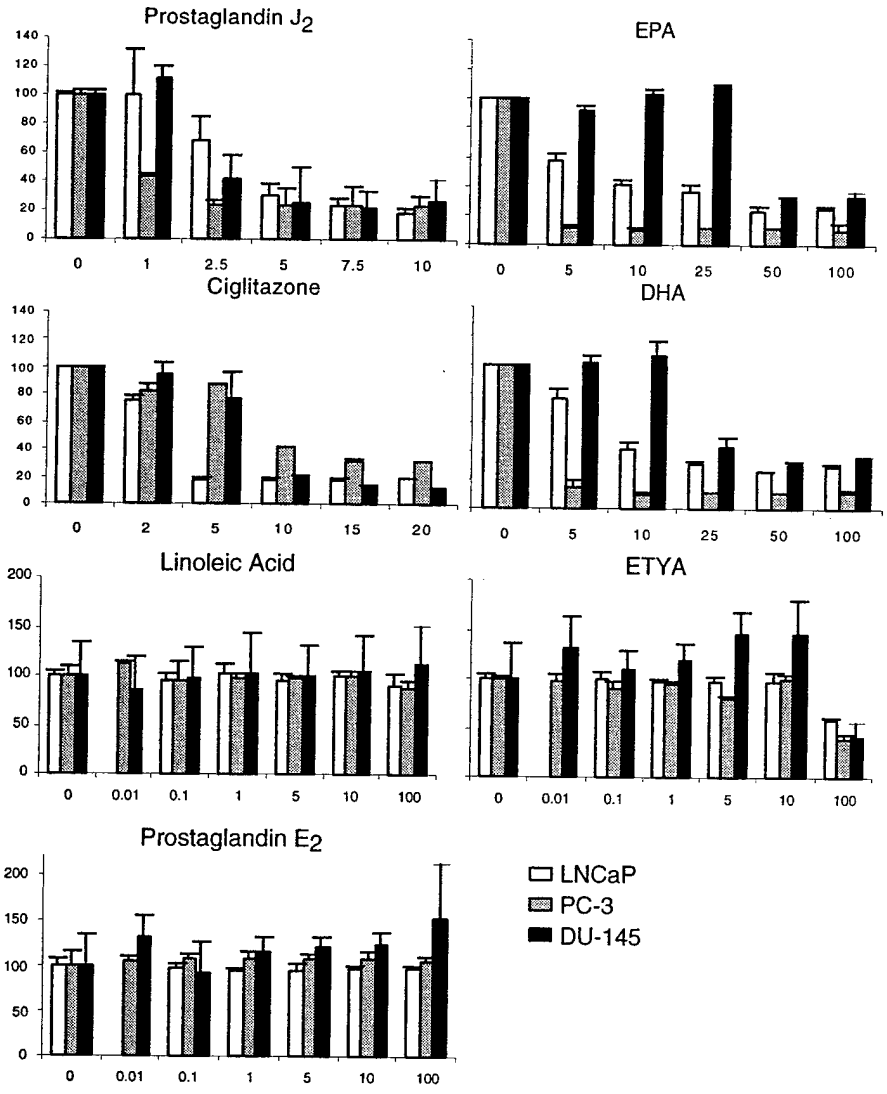

Fig. 1. The effects of activators of PPARs on the viability of human prostatic adenocarcinoma cell lines, DU145, PC-3, and LNCaP. Cells were incubated with 0.01–100 μM linoleic acid (an activator of PPAR-β), ETYA (an activator of PPAR-α), and prostaglandin E_2 (an inert activator for PPARs); 1–10 μM, 15d-PGJ_2; 5–100 μM EPA and DHA; and 2–20 μM, ciglitazone (activators of PPAR-γ); or, vehicle controls (*column 0*) for 6 days. Viable cells were measured by MTS assay and expressed as a percentage of controls (n = 4–6); *bars*, SD.

Although several long-chain fatty acids can activate PPARs, they are not effective activators for PPAR-γ (23–27). However, a fatty acid metabolite, 15d-PGJ_2, the terminal metabolite of the prostaglandin J series, has been shown to be a highly specific activator of PPAR-γ (25, 26). Prostaglandin D_2 and prostaglandin J_2 are endogenous metabolites of the prostaglandin J series that have already been shown to have antitumor activities (11). These observations led us to study the effect of 15d-PGJ_2 on the growth of prostate cancer cells with the hypothesis that the action of these prostaglandins may be occurring through PPAR-γ.

Results

15d-PGJ_2 Inhibits the Growth of Prostate Cancer Cell Lines. Lipids that are known to be specific activators of the three isoforms of PPAR were used to establish the involvement of the particular isoforms in the growth response mechanism in human prostate adenocarcinoma cells. Hormone sensitive (LNCaP) and hormone refractory (PC-3 and DU145) prostate cancer cell lines were treated with ETYA (22, 26), an activator for PPAR-α; linoleic acid (23, 27), an activator for PPAR-β; 15d-PGJ_2 (24, 25), an activator for PPAR-γ; and prostaglandin E_2 (23, 25–27), an inert activator for PPARs over a range of concentrations (1 to 100 μM). Additionally, the synthetic PPAR-γ agonist ciglitazone, as well as two ω-3 polyunsaturated fatty acids, EPA and DHA, which are natural PPAR-γ activators, were included in the studies. The effect of each ligand on the growth response of the cells was determined using the MTS cell viability assay. Neither prostaglandin E_2 nor linoleic acid had any apparent effect on the viability of any of the cell lines examined. ETYA had an inhibitory effect on all three cell lines but only at the highest concentration tested (100 μM; Fig. 1). In comparison, 15d-PGJ_2 showed a potent inhibitory effect (at ~2.5 μM or less) on all cell lines tested (Fig. 1). It is important to note that the effective concentration of 15d-PGJ_2 needed to reduce cell viability (2.5 μM) is comparable with that of 15d-PGJ_2 required for PPAR-γ activation in gene transfer studies (2 μM;

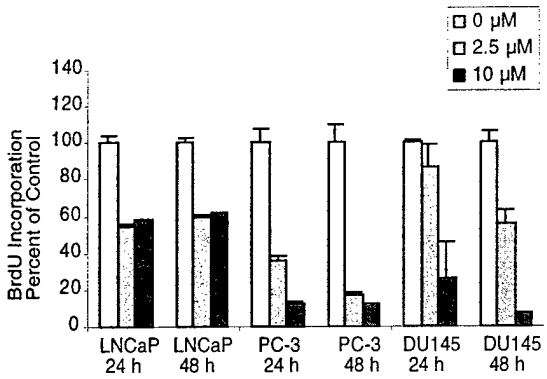

Fig. 2. The effects of 15d-PGJ_2 on prostate cancer cell growth analyzed by DNA synthesis. LNCaP, PC-3, and DU145 cells were treated with 0, 2.5, and 10 μM 15d-PGJ_2 for 24 and 48 h. Additionally, cells were incubated with 10 μM bromodeoxyuridine solution for 18 h prior to harvesting. The amount of newly synthesized DNA was measured by nonradioactive bromodeoxyuridine ELISA (Roche) and expressed as percentage of controls (n = 4); bars, SD.

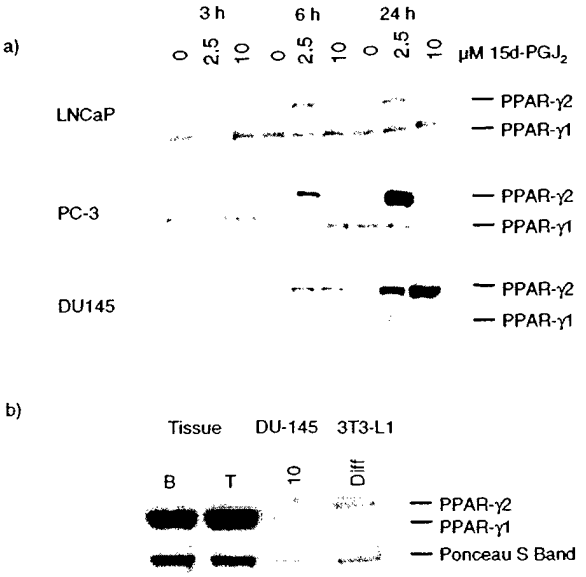

Fig. 3. Expression of PPAR-γ1 and PPAR-γ2 isoforms in human prostate cancer cell lines showing the effect of 15d-PGJ_2 treatment. *a*, cells were treated with 2.5 and 10 μM 15d-PGJ_2 and harvested at 3-, 6-, and 24-h intervals. Western blots were prepared and probed with anti-PPAR-γ antibody (1:2000; BioMol), which detects both isoforms of PPAR-γ. *b*, Western blots of benign (*B*) and cancerous (*T*) prostate tissue, DU145 cells treated with 10 μM 15d-PGJ_2 for 6 h, and differentiated 3T3-L1 cells. The same antibody shown in *a* was used in *b*.

Ref. 25). At higher concentrations of 15d-PGJ_2 (up to 10 μM studied), a profound effect on cell viability was seen. Treatment with EPA, DHA, and ciglitazone also produced a potent growth-inhibitory effect. Ciglitazone produced an inhibitory pattern that was similar to 15d-PGJ_2 at comparable concentrations. However, the concentrations of EPA and DHA needed to produce the effect were much higher than that of 15d-PGJ_2. Transfection studies (28, 29) also show that a higher concentration of EPA and DHA is required for PPAR γ activation, although *in vitro* ligand binding studies demonstrate an affinity (K_d) of ~2 μM for EPA binding. One possible explanation for this is that EPA and DHA have differences in compound stability and binding to fatty acid binding protein compared with 15d-PGJ_2. The transportation of EPA and DHA into cells may be mediated by fatty acid transporters (30).

To confirm the effect of 15d-PGJ_2 on cell proliferation, the incorporation of bromodeoxyuridine into DNA was measured in a nonradioactive DNA synthesis assay. As shown in Fig. 2, treatment with 2.5 and 10 μM 15d-PGJ_2 decreases DNA synthesis significantly in these cells by 24 h. For PC-3 and DU145 cells, DNA synthesis decreased additionally between 24 and 48 h of treatment. Together these two assays suggest that the effect of 15d-PGJ_2 on these cells (also see below) is to induce cell death but not terminal differentiation, as has been suggested for other tumor cell lines (31, 32). In addition, these data show that the end point of the cell death induced by 15d-PGJ_2 is occurring between 24 and 48 h in the majority of cells. However, the initiation of the 15d-PGJ_2 effect occurs very rapidly, with cells starting to round up and detach from the culture dish within 2 h of treatment (data not shown).

Expression of PPARs in Prostate Cancer Cell Lines and Tissues. Because 15d-PGJ_2 is a ligand for PPAR-γ, it is reasonable to expect that this receptor is the mediator for the inhibitory growth effect of 15d-PGJ_2 on prostate cancer cells. Western blotting analysis of total cell extracts from LNCaP, PC-3, and DU145 prostate cancer cell lines using a PPAR-γ-specific polyclonal antibody demonstrated the expression of the receptor in all three human cell lines (Fig. 3*a*). The PPAR-γ antibody clearly recognizes both the γ1 and γ2 isoforms of the receptor. In addition, when cells were treated with low concentrations of 15d-PGJ_2 (2.5 μM) over 24 h, a marked increase in the level of PPAR-γ2 was observed as early as 6 h. By 24 h, an even larger increase in the level of PPAR-γ2 protein had occurred in PC-3 and DU145 cell lines (Fig. 3*a*). Moreover, when DU145 cells were treated at the highest dose of 15d-PGJ_2 (10 μM), a significant increase in the expression of PPAR-γ2 was seen, especially by 24 h of treatment. The expression level of PPAR-γ1 remained unchanged with these treatments and therefore served as an internal control. A Western blot analysis of benign and cancerous prostate tissues was performed to see the expression patterns of PPAR-γ (Fig. 3*b*). Tissues from three different patients were examined, and one representative blot is shown. The analysis showed that PPAR-γ1 protein can be detected in all tissues tested at relatively constant levels, and PPAR-γ2 is not present in these tissues. As controls for PPARγ expression, DU145 cells treated for 6 h with 10 μM 15d-PGJ2 and differentiated 3T3-L1 cells are shown in Fig. 3*b*.

We also carried out Western blot analysis on these cells to determine the expression levels of the α and β isoforms of PPAR. There was no detectable level of expression of either PPAR-α or PPAR-β protein in any of the prostate cancer cell lines studied (data not shown). Taken together, these results suggest that 15d-PGJ_2 has a specific antiproliferative effect on the growth of both androgen-dependent and androgen-independent prostate cancer cell lines, and that this action is occurring through a pathway involving PPAR-γ.

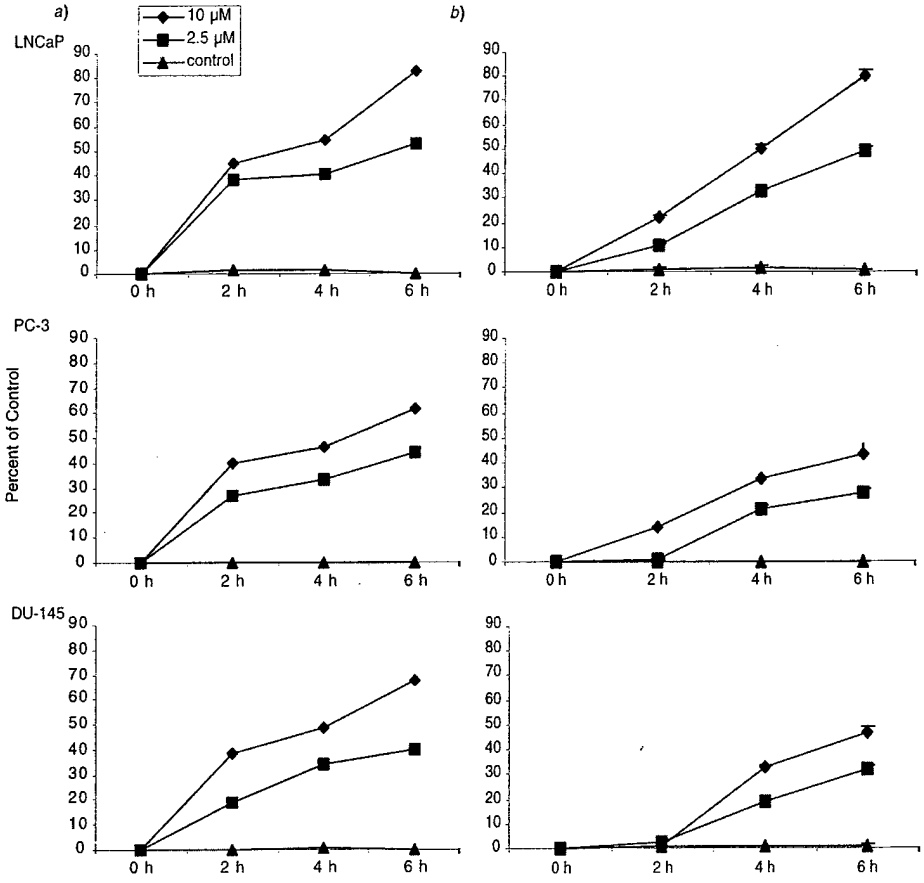

Fig. 4. Effects of 15d-PGJ_2 treatment on plasma membrane integrity assessed by trypan blue exclusion assay and PI staining. LNCaP, PC-3, and DU145 cells treated with 0, 2.5, and 10 μM 15d-PGJ_2 were stained with: *a*, trypan blue dye; or *b*, PI and Hoechst 33258 at 2, 4, and 6 h after treatment. The number of blue (*a*) or red (*b*) cells per total of 500 was counted and expressed as a percentage of the total (n = 4).

Treatment of Prostate Cancer Cells with 15d-PGJ_2 Causes Changes in Plasma Membrane Integrity. We observed that the cells round up in a short time after 15d-PGJ_2 treatment but do not die completely until after 24 h of treatment (data not shown). This suggests that changes may also be occurring at the level of the plasma membrane. Two staining methods were used to assess whether the plasma membranes of cells treated with 15d-PGJ_2 were undergoing permeability changes. Trypan blue staining was performed on cells treated with either 2.5 or 10 μM 15d-PGJ_2 for 2, 4, and 6 h (Fig. 4*a*) and cells treated with 50 μM EPA, 50 μM DHA, and 15 μM ciglitazone at 6 h of treatment. The number of cells staining blue in a total of 500 cells was counted and expressed as a percentage. Fig. 4*a* shows that by 2 h of treatment with both 2.5 and 10 μM 15d-PGJ_2, all three cell lines had a significant number of trypan blue-stained cells compared with controls. LNCaP cells were the most affected by 15d-PGJ_2 treatment in this assay. By 6 h of treatment, ~80% of the LNCaP cells treated with 15d-PGJ_2 are capable of taking up trypan blue dye. The effect of 15d-PGJ_2 occurred in a dose-dependent manner. After 6 h of treatment with EPA, LNCaP, PC-3, and DU145 cells took up 99, 97, and 91% of trypan blue dye, respectively (data not shown). After treatment with DHA, 98, 97, and 95% of LNCaP, PC-3, and DU-145 cells took up trypan blue, respectively (data not shown). After ciglitazone treatment, 59, 92, and 51% of LNCaP, PC-3, and DU145 cells took up trypan blue dye (data not shown). Some cells appeared to be surrounded by a ring of trypan blue dye at the membrane surface. These cells were counted as trypan blue positive and may account for the discrepancy between the number of cells stained by trypan blue and PI (see below).

The second assay involved staining with two DNA-binding dyes, PI and Hoechst 33258, which can be viewed with fluorescence microscopy. In addition to showing nuclear morphology by binding DNA, PI can also be used to determine plasma membrane integrity, because this dye is a polar molecule and cannot enter the cell unless the plasma membrane is perturbed in some manner. In contrast, Hoechst 33258 can freely enter cells and stain DNA to show nuclear morphology. Therefore, these two dyes were used to test the plasma membrane integrity and to visualize any changes in nuclear morphology (see below) at various time points after 15d-PGJ_2 treatment. Staining with PI (Fig. 4*b*) correlated well with trypan blue, taking into account the discrepancy described above. As with the trypan blue staining, 15d-PGJ_2 treatment had a profound effect on the ability of LNCaP cells to take up PI, indicating an effect on the integrity of the plasma membrane. Together, these data suggest that a relatively early effect of the PPAR-γ ligand, 15d-PGJ_2, is to cause disturbances in the plasma membrane, resulting in a loss of integrity and eventually cell death. However, the dis-

Table 1 Cell cycle analysis of prostate cancer cell lines treated with 15d-PGJ_2

Cells were treated with 2.5 and 10 μM 15d-PGJ_2 for 24 and 48 h and then analyzed by FACS. $n = 4$ for 10 μM 15d-PGJ_2 treatment and $n = 2$ for 2.5 μM 15d-PGJ_2 treatment. Values are mean ± SD.

	24 h			48 h		
	G_0/G_1	S	G_2/M	G_0/G_1	S	G_2/M
10 μM J_2 LNCaP	72.48 ± 0.71	10.83 ± 0.07	16.70 ± 0.78	80.48 ± 1.71	5.88 ± 0.24[a]	13.64 ± 1.47
2.5 μM J_2	71.89	9.53	18.59	75.44	7.14	17.43
Control	72.11 ± 2.08	3.83 ± 0.23	24.07 ± 1.86	78.18 ± 0.84	2.11 ± 0.23	19.71 ± 0.62
10 μM J_2	50.43 ± 0.24	36.44 ± 0.55	13.13 ± 0.31	51.27 ± 0.98	33.46 ± 0.40	15.28 ± 1.38
PC-3						
2.5 μM J_2	47.25	31.07	21.69	48.23	37.75	14.03
Control	55.33 ± 0.48	24.52 ± 0.18	20.16 ± 0.6	53.26 ± 0.49	31.66 ± 0.04	15.08 ± 0.45
10 μM J_2	42.04 ± 0.17	25.38 ± 3.10	32.58 ± 3.26	37.00 ± 4.59	34.82 ± 22.7	28.19 ± 18.1
DU145						
2.5 μM J_2	35.89	42.23	21.88	49.85	14.73	35.43
Control	54.67 ± 1.04	20.24 ± 1.17	20.10 ± 0.12	59.15 ± 0.34	4.34 ± 4.57	36.51 ± 4.24

[a] $P \leq 0.05$ *versus* control.

turbance of the plasma membrane may not be a direct effect of 15d-PGJ_2, because this effect occurs gradually and over an extended period of time,.

15d-PGJ_2 Treatment Causes S-Phase Cell Cycle Arrest in Prostate Cancer Cell Lines. Because of the profound inhibition of cellular proliferation caused by 15d-PGJ_2, we wanted to determine whether the cell cycle was altered. LNCaP, PC-3, and DU145 cells were treated with 2.5 and 10 μM 15d-PGJ_2 for 24 and 48 h, at which time cell cycle changes were studied by FACS analysis. All three cell lines showed a significant accumulation of cells in the S-phase by 24 h of treatment with 15d-PGJ_2 compared with control cells (Table 1). However, the androgen-dependent cell line, LNCaP, exhibited a lesser effect than the androgen-independent cell lines DU145 and PC-3; although compared with control cells, there was approximately three times the number of treated cells in S-phase. LNCaP cells grow very slowly in culture and therefore may not have completed an entire cell cycle before the effects of 15d-PGJ_2 occur.

The completion of cell cycle events in an orderly manner, from the G_1 stage to DNA replication in S-phase or from the G_2 stage to mitosis, is controlled by many factors, which act as checkpoints to ensure that no mistakes occur (33). Therefore, in addition to carrying out FACS analysis to study the cell cycle, we also studied changes in the protein expression of certain cell cycle regulating factors over a time course of 15d-PGJ_2 treatment. The cell cycle regulators studied were p53, p21, and p27, all of which are involved in controlling various checkpoints in the cell cycle. However, no changes were observed in the expression levels of any of these proteins over the time period in which cell cycle arrest occurred (data not shown).

After observing the 15d-PGJ_2-induced cell cycle changes mentioned above, we were interested to see whether 15d-PGJ_2 could induce differentiation of prostate cancer cells into adipocytes, as has been described for other cell types. The C/EBPs, C/EBP-α and C/EBP-β, are nuclear transcription factors, which are vital components for the differentiation of preadipocytes into adipocytes (34–37). It has been demonstrated that some compounds, such as the thiazolidinediones (31, 37–39), generally up-regulate the expression of these proteins. When we examined the levels of C/EBP-α and C/EBP-β, there was no effect of 15d-PGJ_2 by 3 h in all cell lines studied (Fig. 5*a*). Moreover, by 6 and 24 h, the levels of both C/EBP-α and C/EBP-β were significantly decreased compared with controls. To confirm that there is no adipocytic program initiated by 15d-PGJ_2 a Northern blot analysis for aP2 was performed (Fig. 5*b*). Differentiated 3T3-L1 cells were used as a positive control. The figure shows that there is no up-regulation of the aP2 mRNA by 15d-PGJ_2 treatment in either LNCaP or DU145 cells. PC-3 cells also exhibited no up-regulation (data not shown). In addition, we tested for the accumulation of neutral lipids with oil red O dye. When LNCaP, PC-3, and DU145 cells were treated for 4 days with a range of concentrations of 15d-PGJ_2, no differences were detected in the amount of oil red O staining between treated cells and controls (data not shown). These results suggest that 15d-PGJ_2 does not induce differentiation of these cells into adipocytes. A Northern blot analysis of PSA was also performed to prove there is no further differentiation with 15d-PGJ2 treatment (Fig. 5*c*). The Northern blot results show that after the up-regulation of PSA by mibolerone in LNCaP cells, 15d-PGJ_2 treatment down-regulates the expression of PSA mRNA.

Cell Death Induced by 15d-PGJ_2 Occurs via a Non-apoptotic Mechanism. A number of apoptotic assays were performed to investigate the mode of cell death occurring in response to 15d-PGJ_2. Nuclear morphology changes, DNA fragmentation, and PARP cleavage were studied at various time points after treatment with 10 μM 15d-PGJ_2. No DNA fragmentation or PARP cleavage, both of which are classic events known to occur during apoptosis, was observed in any of the cell lines (data not shown; Refs. 40 and 41). Moreover, the use of caspase inhibitors to block or delay apoptosis had no effect on the induction of cell death by 15d-PGJ_2 (data not shown). Fig. 6 shows an example of Hoechst 33258 and PI staining of LNCaP cells after 6 h of 10 μM 15d-PGJ_2 treatment. Clearly, none of the nuclear morphology changes associated with apoptosis have occurred by this time point. Ciglitazone treatment also showed no

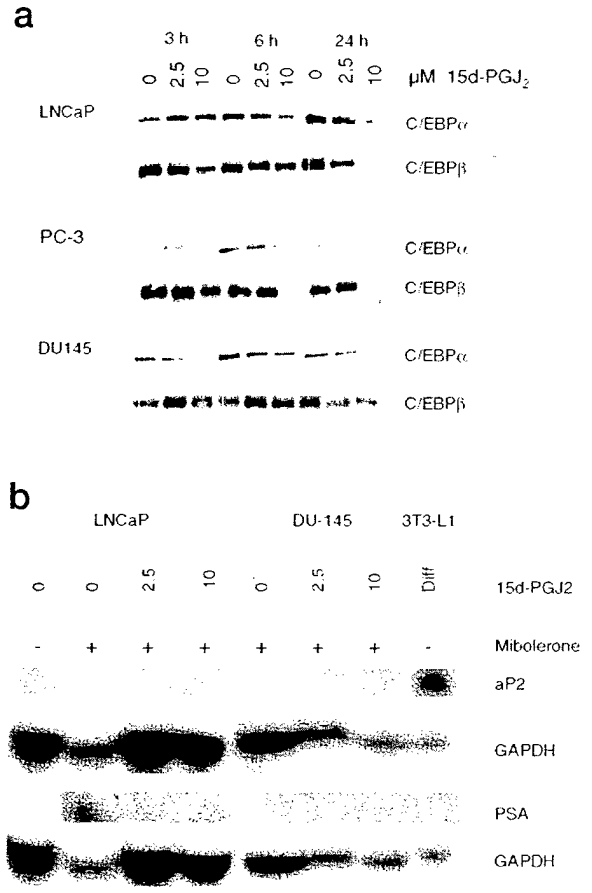

Fig. 5. Expression of differentiation markers. *a,* the expression of C/EBPα and C/EBPβ was studied by Western blotting of LNCaP, PC-3, and DU145 cells treated with 0, 2.5, and 10 μM 15d-PGJ$_2$ for 3, 6, and 24 h. Anti-C/EBPα and anti-C/EBPβ antibodies (1:500; Santa Cruz) were used for immunodetection. *b,* a Northern blot of mRNA in LNCaP, DU145, and differentiated 3T3-L1 cells using a probe for aP2, PSA, and glyceraldehyde-3-phosphate dehydrogenase (*GAPDH*).

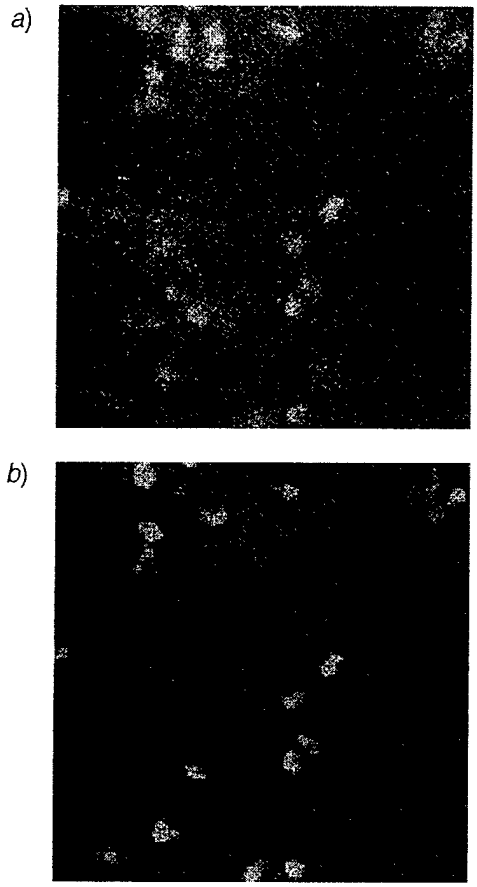

Fig. 6. Nuclear staining of LNCaP cells. LNCaP cells were treated with 10 μM 15d-PGJ$_2$ for 6 h and stained with Hoechst 33258 and PI. Cells were photographed from a double-stained population by confocal microscopy. *a,* Hoechst 33258; *b,* PI.

nuclear morphology changes associated with apoptosis by Hoechst 33258 staining (data not shown). The nuclei from all three cell lines were still intact at 72 h of treatment (data not shown). Moreover, the majority of cells (80%) stained with both PI and Hoechst 33258 (Fig. 6), and the cells with PI staining also had more intense Hoechst 33258 staining, suggesting that the plasma membrane may have become more permeable even after short exposures (6 h) to 15d-PGJ$_2$.

To delineate whether any further alterations in the plasma membrane occurred and to look for additional ultrastructural changes, transmission electron microscopy was performed on cells from all three cell lines treated with 2.5 and 10 μM 15d-PGJ$_2$ for 24 h. Negative control cells received no treatment. Positive controls for necrosis and apoptosis (42, 43) were treated with high (20 μM) and low (2 μM) concentrations of the calcium ionophore A23187, respectively. Electron micrographs of representative cells can be seen in Fig. 7. The majority of cells maintained an intact plasma membrane after treatment with 10 μM 15d-PGJ$_2$ for 24 h, unlike those seen in the necrosis control in which almost all cells have completely disrupted membranes and have lost their cellular contents (Fig. 7*c*). A small percentage of 15d-PGJ$_2$-treated cells also have this morphology, but this is likely to be attributable to mechanical damage incurred while preparing the cells for electron microscopy.

LNCaP, PC-3, and DU145 cells all originate from prostate epithelia and as such have distinct microvilli on their surfaces (particularly clear in DU145 cells). Cells treated with 15d-PGJ$_2$ showed a pronounced loss of plasma membrane microvilli (Fig. 7, compare *b* to *f* and *h*). These changes at the cell surface may be enough to allow the uptake of polar dyes such as PI.

The nuclei of cells remained intact after 15d-PGJ$_2$ treatment in correlation with the Hoechst 33258 nuclear staining and DNA fragmentation data. Chromatin condensation was still evident, although complete segregation has not occurred to give the pyknotic structures seen in apoptotic cells. This can be seen in the apoptosis control cells treated with 2 μM A23187 (Fig. 7*d*).

The cytoplasmic changes seen in cells treated with 15d-PGJ$_2$ are possibly more dramatic than the nuclear events. Cytoplasmic changes included extensive vacuolization and distension of the endoplasmic reticulum (Fig. 7, *e–h*). In a

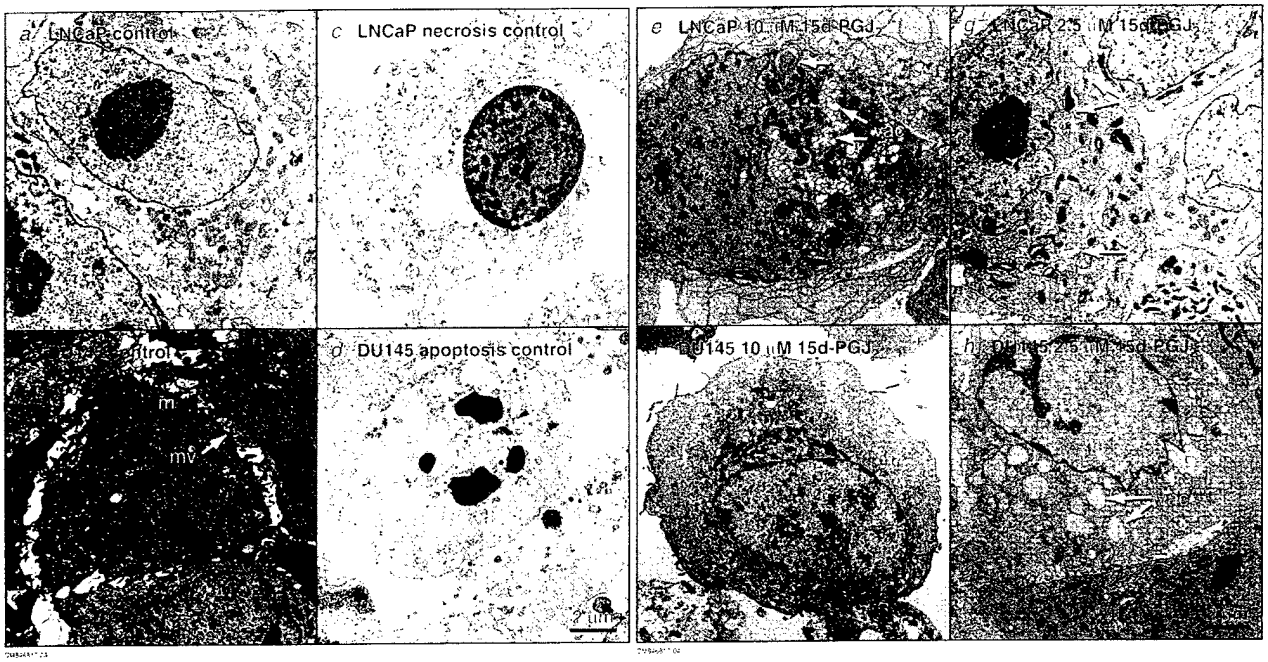

Fig. 7. Transmission electron micrographs showing morphological changes in prostate cancer cells treated with 15d-PGJ_2. *a*, LNCaP control; *b*, DU145 control, note the location of the mitochondria (*m*) throughout the cytoplasm and the extensive microvilli (*mv*) in the plasma membrane; *c*, necrosis control, LNCaP cells treated with 20 μM A23187 for 2 h; *d*, apoptosis control, DU145 cells treated with 2 μM A23187 for 6 h; *e*, LNCaP cells treated with 10 μM 15d-PGJ_2 for 24 h, showing perinuclear position of mitochondria, vacuolization of the cytoplasm (*vac*), and distension of endoplasmic reticulum into autophagic vesicles (*av*); *f*, DU145 cells treated with 10 μM 15d-PGJ_2 for 24 h, showing loss of microvilli (*arrow* with *asterisk*), perinuclear location of mitochondria (*m*) and chromatin condensation; *g*, LNCaP cells treated with 2.5 μM 15d-PGJ_2 for 24 h, showing vacuolization (*vac*), distended endoplasmic reticulum, autophagic vesicles (*av*) and chromatin condensation; and *h*, DU145 cells treated with 2.5 μM 15d-PGJ_2, showing loss of microvilli, chromatin condensation, and extensive vacuolization of the cytoplasm (*vac*).

number of cells, the endoplasmic reticulum was distended to such an extent that "whorl-like" structures formed, and some of these appear to contain organelles, possibly mitochondria, which may be undergoing degradation by autophagy. In addition, a pronounced phenomenon involving the movement of mitochondria from a diffuse cytoplasmic pattern of localization to a tightly packed grouping in a perinuclear position occurred in the majority of cells treated with 10 μM 15d-PGJ_2 (Fig. 7, *e* and *f* compared with *a* and *b*). PC-3 cells showed similar cytoplasmic changes (data not shown).

15d-PGJ_2 Causes a Decrease in Mitochondrial Membrane Potential. The prominent change in mitochondrial position, together with the apparent autophagic degradation of a number of mitochondria in 15d-PGJ_2-treated cells, suggests that mitochondrial function may be impaired in these cells. In addition, changes in plasma membrane integrity can also have a profound effect on the stability of mitochondrial function. Therefore, the mitochondrial abnormalities observed by electron microscopy were evaluated further using a specific fluorescent mitochondrial probe, JC-1. JC-1 is a lipophilic cation that normally exists as a monomer emitting green fluorescence. In a reaction driven by mitochondrial transmembrane potential, JC-1 forms dimeric "J-aggregates" that emit a red fluorescence (44, 45). In this manner, the use of JC-1 enables the dual analysis of mitochondrial mass (green fluorescence) and mitochondrial transmembrane potential (red fluorescence). After treatment with 15d-PGJ_2, we observed a progressive increase in green fluorescence, which correlated with a decrease in red fluorescence at both concentrations of the ligand in all cell lines studied (Fig. 8). As expected, this effect was more profound at 10 μM 15d-PGJ_2 than at the lower concentration. However, at 24 h, the extent of the loss of mitochondrial transmembrane potential inferred by the decreasing red fluorescence and increasing green fluorescence was much greater in PC-3 and DU145 cells than in the LNCaP cell line. These data, together with the red:green fluorescence ratio, which represents the net transmembrane potential per mitochondrion (46), are presented in Table 2. The fact that the profound reduction in mitochondrial transmembrane potential correlates with the time frame in which cell viability is lost after 15d-PGJ_2 treatment suggests that this endogenous ligand for PPAR-γ has a direct effect on mitochondrial function.

Discussion

A principle role for PPAR-γ is to trigger the differentiation cascade resulting in the formation of mature adipocytes from preadipocytes. However, the fact that this receptor is expressed in a variety of normal and tumor tissues suggests an additional role. Because of the antitumor effects observed by other members of the J series of prostaglandins, we were interested in the effect of 15d-PGJ_2 treatment on the growth of prostate cancer cell lines. We also wanted to elucidate whether the mechanism of action was occurring through the PPAR-γ, for which 15d-PGJ_2 is a ligand. In our study, treat-

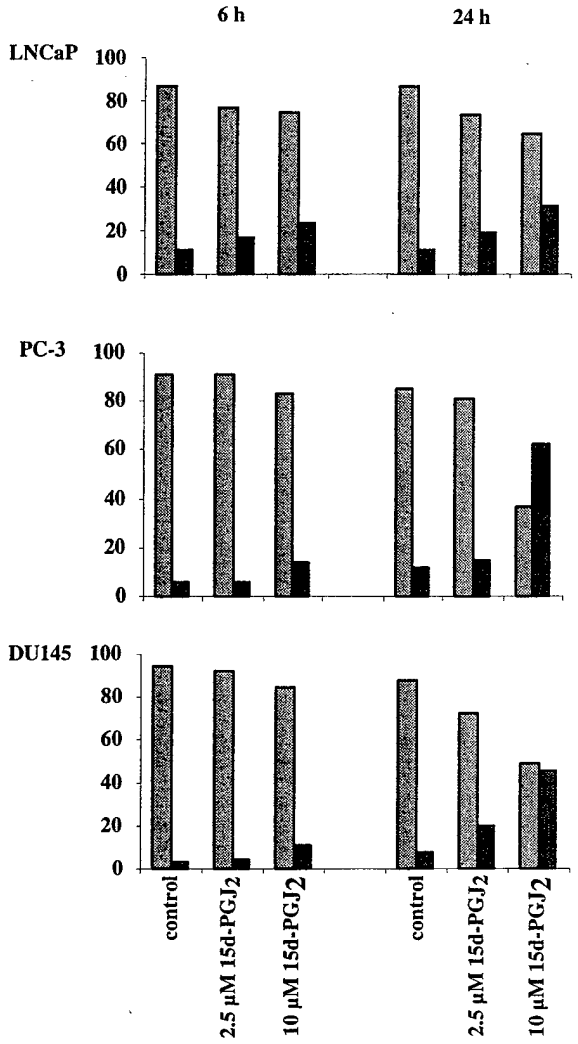

Fig. 8. Effect of 15d-PGJ_2 treatment on the mitochondrial transmembrane potential of prostate cancer cells. LNCaP, PC-3, and DU145 prostate cancer cells were treated with 15d-PGJ_2 for 6 and 24 h. Mitochondrial transmembrane potential was measured using a mitochondria-specific fluorescent probe, JC-1. Red and green fluorescence were measured simultaneously by FACS analysis [excitation at 488 nm; emission 530 nm (green fluorescence) and 585 nm (red fluorescence)]. Events (20,000) were measured, and the number of red or green events is expressed as a percentage of the total (n = 3). $P \leq 0.05$. ▨, red fluorescence; ■, green fluorescence.

ment with 15d-PGJ_2 results in cell death at high and low concentrations in both hormone-sensitive and hormone-resistant human prostate cancer cells.

Our studies have demonstrated that PPAR-γ is expressed in three of the commonly studied metastatic prostate cancer cell lines, LNCaP, PC-3, and DU145 (47), as well as in human benign and cancerous prostatic tissues. Interestingly, we have found that PPAR-γ2 is up-regulated by low concentrations of 15d-PGJ_2 in a time-dependent manner. PPAR-γ2 usually is expressed more specifically in fat cells. However, we could not demonstrate any adipogenic differentiation of treated prostate cancer cells. In addition, at 10 μM of 15d-PGJ_2, PPAR-γ2 was only inducible in DU145 cells. Although the phenomenon seems to be very interesting, no plausible explanation can be offered at the present time. Thus, the role of differentially expressed PPAR-γ2 in prostatic cancer cell death is not clear.

The obvious difference between PPAR-γ2 and PPAR-γ1 is 30 additional amino acids at the NH_2 terminus of the γ2 isoform (18, 19). Werman *et al.* (48) showed that the NH_2 terminus of PPAR-γ2 activates a heterologous promoter to a greater degree than PPAR-γ1. However, the activation domain was mapped to a common region in both isoforms. As for many nuclear receptors, the expression of specific coactivators in a particular cell type has been suggested as a mechanism to confer functional specificity to receptors or isoforms of receptors that bind the same response element. Therefore, it is likely that two isoforms of PPAR-γ are used to enable different factors to regulate their expression and/or activity to meet specific biological requirements. Of the two isoforms, the expression of PPAR-γ2 is influenced more by changes in the nutritional status of an animal, such as obesity or starvation (48). Because we showed that PPAR-γ2 can be differentially regulated by different concentrations of 15d-PGJ_2 in prostate cancer cells, the regulatory mechanisms may deserve further investigation.

Recently, high levels of PPAR-γ were reportedly expressed in prostate cancer tumors (49); therefore the availability of ligand may be an important factor for the action of PPAR-γ as a negative regulator of prostate cancer cell growth. Production of certain prostaglandins may be modulated by the amount of ω-3 *versus* ω-6 fatty acids ingested in the diet. Although the amount of 15d-PGJ_2 in the prostate has not been determined, the prostate gland does produce large amounts of prostaglandins (50–52). In fact, the prostate has the capacity to produce prostaglandin D_2, which can be spontaneously converted to 15d-PGJ_2, the terminal metabolite of this prostaglandin series (53). Therefore, the modulation of 15d-PGJ_2 via "good" fat in the diet presents a novel therapeutic and potential preventive method for treating prostate cancer. However, PPAR-γ can be activated by a number of ligands; therefore, the level of 15d-PGJ_2 alone may not be as important as the total amount of available ligand.

PPAR-γ is known to cause cell cycle withdrawal preceding adipocyte differentiation (54). Cell cycle withdrawal in preadipocytes correlates with a large decrease in the DNA binding and transcriptional activity of E2F/DP, a growth-related transcription factor. Because the discovery of natural and synthetic ligands for PPAR-γ, a potential therapy for a number of cancers has been suggested. This therapy uses a mechanism of growth inhibition by terminal differentiation of the cancer cells into adipocytes via PPAR-γ activation. Although this theory has shown potential in breast and liposarcoma cancers (31–32, 55), we and others have found no evidence that terminal differentiation is occurring in prostate cancer cells (49). However, the accumulation of cells in the S-phase of the cell cycle after 15d-PGJ_2 treatment (more pronounced for PC-3 and DU145 cell lines) was unexpected. Because other members of the prostaglandin J series have been shown to cause G_1 arrest at lower doses and at higher concentrations cause G_2-M arrest leading to apoptosis, we

Table 2 Mean fluorescence values of mitochondrial mass and $\Delta\psi_m$ in 15d-PGJ_2-treated cells (relative to control cells)

Green and red fluorescence are expressed as a ratio of treated:control. Decreasing red fluorescence indicates a loss of mitochondrial transmembrane potential in correlation with increasing green fluorescence ratio.

	10 μM 15d-PGJ_2		2.5 μM 15d-PGJ_2	
	6 h	24 h	6 h	24 h
JC-1 red	0.87 ± 0.04[a]	0.74 ± 0.05[a]	0.89 ± 0.04[a]	0.85 ± 0.01[a]
LNCaP				
JC-1 green	2.16 ± 0.44[a]	2.19 ± 0.35[a]	1.59 ± 0.26[a]	1.73 ± 0.20[a]
Red/green	0.4 ± 0.11[a]	0.25 ± 0.05[a]	0.56 ± 0.13[a]	0.49 ± 0.07[a]
JC-1 red	0.91 ± 0.03[a]	0.43 ± 0.03[a]	1 ± 0.02	0.96 ± 0.05
PC-3				
JC-1 green	2.34 ± 0.58[a]	5.28 ± 0.57[a]	0.97 ± 0.13	1.28 ± 0.18
Red/green	0.39 ± 0.12[a]	0.08 ± 0.01[a]	1.03 ± 0.16	0.75 ± 0.19
JC-1 red	0.89 ± 0.01[a]	0.56 ± 0.03[a]	0.98 ± 0.01[a]	0.83 ± 0.08[a]
DU145				
JC-1 green	4.07 ± 0.62[a]	5.53 ± 0.52[a]	1.49 ± 0.47	2.4 ± 0.85[a]
Red/green	0.22 ± 0.04[a]	0.1 ± 0.01[a]	0.66 ± 0.19[a]	0.35 ± 0.20[a]

[a] $P \leq 0.05$ *versus* control.

thought similar events would occur with 15d-PGJ_2 treatment (56, 57). Many assays used to detect apoptotic events showed that this was not the case. In fact, the effect of 15d-PGJ_2 on prostate cancer cells is the induction of rapid detachment of the cells by 6 h of treatment and ending with the majority of cells dead at 24 h.

PI and trypan blue staining assays showed that polar dyes were able to be taken up by a large majority of the cells at about the same time that detachment from the culture dish was occurring, which taken alone could be indicative of necrosis. Studies at the electron microscopy level showed that many of the typical signs of necrosis are not occurring in these prostate cancer cells treated with 15d-PGJ_2. In fact, many of the morphological changes occurring in these cells as a result of 15d-PGJ_2 treatment, for example, loss of microvilli, vacuolization of the cytoplasm, chromatin condensation without nuclear fragmentation, and loss of cytoplasmic structures are indicative of type 2 (autophagic) programmed cell death (58). This form of cell death is characterized primarily by the formation of autophagic vacuoles, together with the occasional dilation of mitochondria and endoplasmic reticulum (59, 60). Although autophagic vacuoles were seen in only a small percentage of cells treated with 15d-PGJ_2, dilated endoplasmic reticulum was observed in almost all cells. Autophagy does not directly destroy the plasma membrane (by definition) or the intact nucleus, probably because of its size. However, plasma membrane changes are seen in cells undergoing autophagic cell death. This is more pronounced in epithelial cells that lose microvilli and/or junctional complexes (60–63) and can clearly be seen to occur in our cell culture system upon treatment with 15d-PGJ_2. This may account for the loss of plasma membrane integrity inferred by the uptake of PI and trypan blue dyes. The nuclear degradation reported in autophagic cell death is by no means as prevalent or striking as that seen in apoptosis, although in some cases of these types of cell death pyknotic nuclei are reported (60, 64). In all cases, the nuclei of the treated cells in our study remained intact, although a certain amount of chromatin condensation was seen to occur. The lack of DNA fragmentation after nuclear condensation in these cells suggests that they may already have lost their ATP because of decreased mitochondrial function (see below) and plasma membrane integrity. Therefore, they are not able to further process chromatin, which requires energy, and proceed along the apoptotic pathway (65).

One interpretation of the role of autophagy is that it protects the cell rather than destroying it by degrading restricted parts of the cytoplasm through autolysis and segregation, thus protecting the rest of the cell (59). This protective mechanism may be occurring in these prostate cancer cells treated with 15d-PGJ_2 because this treatment also induces the expression of heat shock protein 70,[5] which plays a role in the stress response of cells and may be up-regulated in an attempt to evade death (66–69).

For many years, it has been known that mitochondria play a central role in the mechanism of necrotic cell death, but only recently has this role been extended to include apoptosis (reviewed in Refs. 70 and 71). Although we believe that the mechanism of cell death occurring in our system is neither necrosis nor apoptosis, the involvement of mitochondria in the mechanism of cell death cannot be ruled out. Mitochondria are the primary organelles targeted for autophagy in type 2 cell death and appear to be engulfed by dilated endoplasmic reticulum in some of the cells in our study. Therefore, we looked at the functioning of mitochondria after treatment with 15d-PGJ_2 by studying their transmembrane potential. JC-1 is a fluorogenic molecule widely used for the purpose of measuring mitochondrial transmembrane potential (44, 45). Treatment with 15d-PGJ_2 does indeed greatly reduce the mitochondrial transmembrane potential in all three cell lines, starting at 6 h of treatment. By 24 h, the effect is greatly pronounced, particularly in DU145 and PC-3 cells. It has been shown that the expression of an important group of proteins, the uncoupling proteins, involved in the uncoupling of oxidative phosphorylation from ATP synthesis, is regulated by PPAR-γ. The uncoupling pro-

[5] R. Butler and C. Y-F. Young, unpublished observation.

teins are transmembrane proteins found in the inner mitochondrial membrane, predominantly in brown adipose tissue and skeletal muscle (72). Whether these uncoupling proteins play a role in the decreased mitochondrial transmembrane potential observed in our cells remains a subject of ongoing investigation in our laboratory.

In addition to decreased mitochondrial function in cells after 15d-PGJ_2 treatment, we also observed the clustering of mitochondria in a perinuclear position rather than the dispersed cytoplasmic distribution as seen in control cells. Mitochondria and microtubules have long been documented to colocalize in many cell types (reviewed in Ref. 73). The involvement of microtubules in the positioning of mitochondria is supported by evidence that mitochondria redistribute in mammalian cells treated with microtubule destabilizing agents (74, 75). The microtubule-based motor proteins, kinesin and cytoplasmic dyenin, bind microtubules and transduce chemical energy into mechanical work as they hydrolyze ATP to enable polarized movement of "cargo" along microtubules (76). Recently, disruption of kinesin motor activity has been shown to cause a perinuclear pattern of mitochondrial localization attributable to the loss of polarized movement to the periphery of the cell (77, 78). Therefore, we suggest that 15d-PGJ_2 may affect mitochondrial functioning by causing mitochondrial membrane depolarization, leading to the uncoupling of oxidative phosphorylation from ATP synthesis and ultimately to cell death.

In summary, we demonstrate that a ligand for PPAR-γ, 15d-PGJ_2, induces nonapoptotic cell death in human prostate cancer cells. We suggest that PPAR-γ is a negative regulator of prostate cancer cell growth. It is apparent from our studies that both mitochondrial and plasma membrane disturbances are involved in the mechanism of cell death. However, further investigation into the downstream events activated by PPAR-γ to induce cell death is required if modulation of ligands for this receptor is to form a significant means of preventing or treating prostate cancer.

Materials and Methods

Cell Culture

LNCaP, DU145, PC-3, and 3T3-L1 cells were obtained from the American Type Culture Collection. All cells were maintained in a humidified atmosphere of 95% air and 5% CO_2 at 37°C. Cells (7.5×10^4 per ml) were seeded in 24-well culture plates in RPMI 1640 supplemented with 5% serum and incubated for 3 days. The medium was changed to serum-free/phenol red-free RPMI 1640 24 h prior to treatment. To differentiate 3T3-L1 cells (79), the cells were treated with 0.25 μM dexamethasone, 0.5 mM 1-methyl-3-isobutylxanthine, and 1 μg/ml insulin. After 48 h, cells were switched to 10% FCS medium containing 1 μg/ml insulin. Then cells were collected, as described below, for Western blotting.

Chemicals

All prostaglandins and fatty acids were purchased from Sigma Chemical Co. (St. Louis, MO) with the exception of 15d-PGJ_2 (Caymen Chemicals, Ann Arbor, MI) and ciglitazone (Biomol, Plymouth Meeting, PA). Stock solutions were prepared and stored according to the manufacturer's specifications.

Assays of Growth Inhibition

Cell Viability Assay. After treatment with ligands at varying concentrations (described in the text), the cells were incubated for an additional 6 days. Cell viability was determined using the MTS colorimetric assay (Promega, Madison, WI). MTS assay reagents (mixed at 1 part phenazine methosulfate to 20 parts MTS, according to manufacturer's instructions) were added to the culture medium at a 1:6 dilution (200 μl/well for 24-well plates and 20 μl/well for 96-well plates). The cells were incubated for 90 min at 37°C, and the absorbance was measured at 490 nm using a plate reader (80, 81). Each experiment was carried out in quadruplicate and repeated at least three times.

DNA Synthesis Assay. Cell proliferation was determined by measurement of bromodeoxyuridine incorporation during DNA synthesis via a nonradioactive colorimetric assay (Ref. 82; Roche, Indianapolis, IN). Cells were treated with 2.5 and 10 μM 15d-PGJ_2, and the amount of bromodeoxyuridine incorporation over an 18-h period was measured at 24 and 48 h. The assay was carried out according to the manufacturer's instructions. The substrate reaction was measured without stop solution at a wavelength of 370 nm on an ELISA plate reader.

Staining Assays for Cell Death and Plasma Membrane Integrity

For all staining assays, cells were treated with 2.5 and 10 μM 15d-PGJ_2, stained, and counted at 2, 4, and 6 h.

PI Staining. Stock solutions of PI (Sigma; 1 mg/ml) were dissolved in PBS and stored at 4°C. Cells were incubated with PI at a final concentration of 1 μg/ml for 5 min at 37°C.

Hoechst 33258 Staining. Stock solutions of Hoechst 33258 (Sigma; 10 mg/ml) were dissolved in PBS and stored at −20°C. Cells were incubated with Hoechst 33258 at a final concentration of 5 μg/ml for 5 min at 37°C. Cells were washed gently with PBS, and red cells (PI) or blue cells (Hoechst 33258) were visualized by fluorescence microscopy using an Axiophot microscope (Zeiss, Inc.). Appropriate excitation filters were used (PI: 546 nm excitation and 590 nm emission; Hoechst 33258: 365 nm excitation and 420 nm emission). The number of red cells per 500 blue cells was counted and expressed as a percentage of the total.

Trypan Blue Staining. Adherent cells were harvested by trypsinization and collected by centrifugation. Nonadherent cells were collected from spent media by centrifugation. Cell pellets were resuspended in 100 μl of fresh media, and trypan blue solution (Sigma) was added at a ratio of 1:1. Blue cells were counted as a percentage of a total of 500 cells.

Western Blotting. Total cell lysates were prepared from each cell line after treatment with 15d-PGJ_2. Adherent and nonadherent cells were collected by low-speed centrifugation and washed with PBS. Cell pellets were gently resuspended in RIPA buffer [PBS containing 1% NP-40, 0.5% sodium deoxycholate, 0.1% SDS plus freshly added protease inhibitors, 100 μg/ml phenylmethylsulfonyl fluoride, 30 μl/ml aprotinin (from Sigma stock solution), and 1 mM sodium orthovanadate]. Benign and cancerous tissues were homogenized in RIPA buffer. All samples were disrupted and homogenized by passage through a 21-gauge needle and incubated for 30 min on ice. Additional phenylmethylsulfonyl fluoride was added to a final concentration of 100 μg/ml. Samples were centrifuged for 20 min at $15,000 \times g$ in a microcentrifuge at 4°C, and the supernatants (total cell lysates) were collected and stored at −20°C. Protein concentration was determined using a detergent-compatible protein assay (Bio-Rad, Hercules, CA), according to the manufacturer's instructions. Equivalent amounts of protein were separated in precast SDS-polyacrylamide gels (Novex, San Diego, CA) and transferred to nitrocellulose membranes (Bio-Rad). Transfer and protein loading were checked by Ponceau S staining prior to blocking the membrane with 5% milk/TBS-Tween 20 (1 h at room temperature). Blocked membranes were incubated overnight with either anti-PPAR-γ polyclonal antibody (BioMol, Plymouth Meeting, PA; 1:2000 dilution), anti-C/EBPα polyclonal antibody (Santa Cruz; 1:500 dilution), or anti-C/EBPβ polyclonal antibody (Santa Cruz; 1:500 dilution). Three 10-min washes in TBS-Tween 20 (20 mM Tris-HCl, 137 mM NaCl, and 0.1% Tween 20, pH 7.6) were carried out between antibody steps, followed by incubation with antirabbit secondary antibody conjugated to horseradish peroxidase (Amersham, Arlington Heights, IL; 1:2000 dilution) for 1 h at room temperature. Immunoreactivity was detected using the enhanced chemiluminescence development method (Renaissance; DuPont NEN, Boston, MA).

Cell Cycle Analysis. Cell cycle analysis was performed on cells treated with 2.5 and 10 μM 15d-PGJ_2 for 24 and 48 h. Adherent and nonadherent cells were collected by centrifugation, washed with PBS, and fixed in 95% ethanol for 10 min on ice. The cells were pelleted, washed

with PBS, and resuspended in 20 μg/ml PI in PBS containing 200 μg/ml RNase. Samples were incubated for 1 h at 37°C and subjected to FACS analysis (Becton Dickinson, Bedford, MA).

Northern Blotting. Cells were treated with varying amounts of 15d-PGJ_2 and 1 nM mibolerone as indicated, and RNA was collected by the guanidinium isothiocyanate method (83). An RNA gel was run and transferred onto a nylon membrane according to the GeneScreen protocol by New England Nuclear. Twenty μg of total RNA were loaded in each lane. cDNAs for PSA, aP2, and glyceraldehyde-3-phosphate dehydrogenase were used as probes labeled with [P^{32}]dCTP by random priming. The hybridization was performed by prehybridizing the membranes for 4 h with a hybridization buffer containing 7% SDS, 1 mM EDTA, and 0.25 M sodium phosphate, pH 7.2. The probes were added to fresh buffer and hybridized overnight. The membranes were washed with a washing buffer containing 0.1× SSC + 0.1% SDS. The films were autoradiographed at −70°C.

Oil Red O Staining. Oil red O staining of neutral lipid accumulation within cells was measured using a spectrophotometric method (84). Cells were grown in 24-well plates and treated with a range of concentrations of 15d-PGJ_2 and incubated at 37°C for 4 days. Nonadherent cells were pelleted by centrifugation in a centrifuge with adaptors for 24-well plates. The medium was removed, and cells were fixed in 3% paraformaldehyde for 1 h at 4°C. Cells were washed with PBS and stained with a 0.5% solution of oil red O (dissolved in methanol and filtered) for 15 min at room temperature. Cells were washed with PBS, and oil red O was extracted by addition of 200 μl isopropanol. The extracted samples were transferred to a clean, 96-well plate, and the absorbance was measured at 510 nm using an ELISA plate reader. The experiment was carried out in quadruplicate and repeated at least three times.

Characterization of Nuclear Morphology. Cells (7.5×10^4 per ml) were seeded onto 10-cm dishes and incubated as above. After 24 h in serum-free/phenol red-free medium, cells were treated with 10 μM 15d-PGJ_2 and incubated for 48 h. The cells were collected by centrifugation, washed twice with PBS, and fixed for 5 min at 4°C with 3% paraformaldehyde in PBS. The cells were collected and resuspended in H_2O for 1 min for rehydration and repelleted. The cells were stained with 0.3 μg/ml Hoechst 33258 for 5 min at room temperature. The stained cells were centrifuged and washed once with PBS and resuspended in an appropriate volume of PBS (200 μl; Ref. 85). The stained nuclei were viewed by fluorescent microscopy using an Axiophot microscope (Zeiss, Inc.). Appropriate excitation filters were used (365 nm excitation; 420 nm emission).

DNA Fragmentation Gel Electrophoresis. DNA fragmentation in cells treated with 2.5 and 10 μM 15d-PGJ_2 was analyzed by gel electrophoresis at 24-, 48-, and 72-h time points using the method of Gunji *et al.* (86). Adherent and nonadherent cells were collected by scraping, followed by centrifugation at 1000 rpm for 10 min. The cell pellets were resuspended in 20 μl of 50 mM Tris-HCl (pH 8.0), 10 mM EDTA, and 0.5 mg/ml proteinase K solution and incubated for 1 h at 50°C. RNase A solution (10 μl of a 0.5 μg/ml stock) was added, and the samples were incubated for 1 h at 50°C. Samples were loaded onto a 1% (w/v) agarose gel after addition of 10 μl of preheated (70°C) loading buffer containing 10 mM EDTA (pH 8.0), 1% (w/v) low-melting point agarose, 0.25% (w/v) bromphenol blue, and 40% (w/v) sucrose. The wells were sealed with 1% (w/v) low-melting point agarose prior to the addition of running buffer to the tank. Samples were electrophoresed at 25 V overnight at 4°C. DNA was visualized by ethidium bromide staining.

Analysis of PARP Cleavage. Cell lysates from 15d-PGJ_2-treated cells were prepared according to the method of Shah *et al.* (87) with minor modifications. Cells were harvested at various time points, collected by centrifugation, and washed with PBS. Repelleted cells were lysed in sample buffer [62.5 mM Tris-HCl (pH 6.8), 6 M urea, 10% glycerol, 2% SDS, 0.00125% bromphenol blue, and 5% β-mercaptoethanol, freshly added]. Analysis of the M_r 116,000 PARP protein and its M_r 89,000 cleavage product was carried out by separation on 8% SDS-PAGE gels, followed by Western blotting, as described above. Anti-PARP polyclonal antibody (1:2000 dilution; Roche) was used to visualize specific bands.

Inhibition of Caspase Activity. Cells were treated with a caspase inhibitor, over a range of concentrations (10–200 μM), for 1 h prior to treatment with 5 and 10 μM 15d-PGJ_2. The caspase inhibitor used was Z-Val-Ala-DL-Asp-fluoromethylketone dissolved in DMSO (Bachem, Torrance, CA; Ref. 88). Inhibition of cell death was assessed by the MTS assay at various time points as described previously.

Transmission Electron Microscopy. Cells were treated with 2.5 and 10 μM 15d-PGJ_2 for 24 h prior to preparation for electron microscopy. Apoptosis and necrosis control samples were prepared by treating the cells with the calcium ionophore A23187 for 2 h at 2 and 20 μM, respectively. Cells were rinsed in warm PBS, harvested by gentle scraping, and pelleted by centrifugation. Cell pellets were resuspended in Trump's fixative (1% gluteraldehyde and 4% formaldehyde in 0.1 M phosphate buffer, pH 7.2; Ref. 89), preheated to 37°C for 1 h at room temperature. Pelleted cells were rinsed three times with 0.1 M phosphate buffer (pH 7.2) and incubated in 1% osmium tetraoxide (phosphate buffered) for 1 h. Cells were washed with rinse buffer, followed by three washes with double-distilled H_2O. Samples were incubated with 1% uranyl acetate for 1 h at room temperature, dehydrated in graded ethanol, infiltrated, and embedded in 100% Spurr's resin (90). Thin (90-nm) sections were cut on a Reichert Ultracut E ultramicrotome, placed on mesh copper grids, and stained with lead citrate. Micrographs were taken on a JEOL 1200 EXII transmission electron microscope (JEOL, Peabody, MA) operating at 60 kV.

Mitochondrial Membrane Potential Analysis. Mitochondrial function was assessed indirectly by measuring the variation in mitochondrial transmembrane potential measured by JC-1 (Molecular Probes, Eugene, OR) red fluorescence using flow analysis (44, 45). Both red and green fluorescence emissions were analyzed after JC-1 staining using the method of Mancini *et al.* (46). Cells treated with 2.5 and 10 μM 15d-PGJ_2 for 6 and 24 h were collected by trypsinization, followed by centrifugation. Cell pellets were resuspended in 500 μl of medium containing 10 μg/ml JC-1 and incubated for 10 min at 37°C before flow analysis. FACScan (Becton Dickinson, Bedford, MA) was used to establish size gates and exclude cellular debris. For each experimental time point, 15d-PGJ_2-treated and control cells were analyzed. The excitation wavelength was 488 nm. The emission wavelengths were 530 nm for green fluorescence and 585 nm for red fluorescence. Events (20,000) were analyzed per sample, and the relative change in mean fluorescence was calculated as the ratio of the 15d-PGJ_2-treated to control samples.

References

1. Pienta, K. J., and Esper, P. S. Risk factors for prostate cancer. Ann. Intern. Med., *118:* 793–803, 1993.

2. Scardino, P. T. Problem of prostate cancer. J. Urol., *152:* 1677–1678, 1994.

3. Walsh, P. C. Prostate cancer kills: strategy to reduce deaths. Urology, *44:* 463–466, 1994.

4. Armstrong, B., and Doll, R. Environmental factors and cancer incidence and mortality in different countries, with special reference to dietary practices. Int. J. Cancer, *15:* 617–631, 1975.

5. Giovannucci, E., Rimm, E. B., Colditz, G. A., Stampfer, M. J., Ascherio, A., Chute, C. C., and Willett, W. C. A prospective study of dietary fat and risk of prostate cancer. J. Natl. Cancer Inst., *85:* 1571–1579, 1993.

6. Pienta, K. J., and Esper, P. S. Is dietary fat a risk factor for prostate cancer? J. Natl. Cancer Inst., *85:* 1538–1540, 1993.

7. Rose, D. P., and Connolly, J. M. Dietary fat, fatty acids and prostate cancer. Lipids, *27:* 798–803, 1992.

8. Pandalai, F. K., Pilat, M. J., Yamazaki, K., Naik, H., and Pienta, K. J. The effects of omega-3 and omega-6 fatty acids on *in vitro* prostate cancer growth. Anticancer Res., *16:* 815–820, 1996.

9. Flanders, W. D. Review. Prostate cancer epidemiology. Prostate, *5:* 621–629, 1984.

10. Wang, Y., Corr, J. G., Thaler, H. T., Tao, Y., Fair, W. R., and Heston, W. D. W. Decreased growth of established human prostate LNCaP tumors in nude mice fed a low-fat diet. J. Natl. Cancer Inst., *87:* 1456–1462, 1995.

11. Fukushima, M. Prostaglandin J_2: anti-tumor and anti-viral activities and the mechanisms involved. Eicosanoids, *3:* 189–199, 1990.

12. Chaudry, A. A., Wahle, K. W. J., McClinton, S., and Moffat, L. E. F. Arachidonic acid metabolism in benign and malignant prostatic tissue *in vitro*: effects of fatty acids and cyclooxygenase inhibitors. Int. J. Cancer, *57:* 176–180, 1994.

13. Robertson, R. P. Prostaglandins and other arachidonic acid metabolites. *In:* K. L. Becker (ed.), Principles and Practice of Endocrinology and

Metabolism, Ed. 2, pp. 1466–1472. Philadelphia: J. B. Lippincott Co., 1995.

14. Harvei, S., Bjerve, K. S., Tretli, E., Robsahm, T. E., and Vatten, L. Prediagnostic level of fatty acids in serum phospholipids: ω-3 and ω-6 fatty acids and the risk of prostate cancer. Int. J. Cancer, *71:* 545–551, 1997.

15. Mangelsdorf, D. J., Thummel, C., Beato, M., Herrlich, P., Schütz, G., Umesono, K., Blumberg, B., Kastner, P., Mark, M., Chambon, P., and Evans, R. M. The nuclear receptor superfamily: the second decade. Cell, *83:* 835–839, 1995.

16. Mangelsdorf, D. J., and Evans, R. M. The RXR heterodimers and orphan receptors. Cell, *83:* 841–850, 1995.

17. Fajas, L., Auboeuf, D., Raspe, E., Schoonjans, K., Lefebvre, A. M., Saladin, R., Najib, J., Laville, M., Fruchart, J. C., Deeb, S., Vidal-Puig, A., Flier, J., Briggs, M. R., Staels, B., Vidal, H., and Auwerx, J. The organization, promoter analysis, and expression of the human *PPARγ* gene. J. Biol. Chem., *272:* 18779–18789, 1997.

18. Tontonoz, P., Erding, H., Graves, R. A., Budavri, A. I., and Spiegelman, B. M. mPPARγ2: tissue specific regulator of and adipocyte enhancer. Genes Dev., *8:* 1224–1234, 1994.

19. Zhu, Y., Qi, C., Korenberg, J. R., Chen, X. N., Noya, D., Rao, M. S., and Reddy, J. K. Structural organization of mouse peroxisome proliferator-activated receptor γ (mPPARγ) gene: alternative promoter use and different splicing yield two mPPARγ isoforms. Proc. Natl. Acad. Sci. USA, *92:* 7921–7925, 1995.

20. Elbrecht, A., Chen, Y., Cullinan, C. A., Hayes, N., Leibowitz, M. D., Moller, D. E., and Berger, J. Molecular cloning, expression and characterization of human peroxisome proliferator-activated receptors γ1 and γ2. Biochem. Biophys. Res. Commun., *224:* 431–437, 1996.

21. Vidal-Puig, A., Jimenez-Linan, M., Lowell, B. B., Hamann, A., Hu, E., Spiegelman, B., Flier, J. S., and Moller, D. E. Regulation of *PPARγ* gene expression by nutrition and obesity in rodents. J. Clin. Investig., *97:* 2553–2561, 1996.

22. Gelman, L., Fruchart, J. C., and Auwerx, J. An update on the mechanisms of action of the peroxisome proliferator-activated receptors (PPARS) and their roles in inflammation and cancer. Cell. Mol. Life Sci., *55:* 932–943, 1999.

23. Mukherjee, L., Jow, L., Croston, G. E., and Paterniti, J. R. Identification, characterization, and tissue distribution of human peroxisome proliferator-activated receptor (PPAR) isoforms PPAR-γ2 *versus* PPAR-γ1 and activation with retinoid X receptor agonists and antagonists. J. Biol. Chem., *272:* 8071–8076, 1997.

24. Vidal-Puig, A. J., Considine, R. V., Jimenez-Linan, M., Werman, A., Pories, W. J., Caro, J. F., and Flier, J. S. Peroxisome proliferator-activated receptor gene expression in human tissues. Effects of obesity, weight loss, and regulation by insulin and glucocorticoids. J. Clin. Investig., *99:* 2416–2422, 1997.

25. Forman, B. M., Tontonoz, P., Chen, J., Grun, R. P., Spiegelman, B. M., and Evans, R. M. 15-Deoxy-$\Delta^{12,14}$-prostaglandin J_2 is a ligand for the adipocyte determination factor PPARγ. Cell, *83:* 803–812, 1995.

26. Kliewer, S. A., Lenhard, J. M., Willson, T. M., Patel, I., Morris, D. C., and Lehmann, J. M. A prostaglandin J_2 metabolite binds peroxisome proliferator-activated receptor γ and promotes adipocyte differentiation. Cell, *83:* 813–819, 1995.

27. Yu, K., Bayona, W., Kallen, C. B., Harding, H. P., Ravera, C. P., McMahon, G., Brown, M., and Lazar, M. A. Differential activation of peroxisome proliferator-activated receptors by eicosanoids. J. Biol. Chem., *270:* 23975–23983, 1995.

28. Yu, K., Bayona, W., Kallen, C. B., Harding, H. P., Ravera, C. P., McMahon, G., Brown, M., and Lazar, M. A. Differential activation of peroxisome proliferator-activated receptors by eicosanoids. J. Biol. Chem., *270:* 23975–23983, 1995.

29. Forman, B. M., Chen, J., and Evans, R. M. Hypolipidemic drugs, polyunsaturated fatty acids, and eicosanoids are ligands for peroxisome, proliferator-activated receptors alpha and delta, Proc. Natl. Acad. Sci. USA, *94:* 4312–4317, 1997.

30. Jump, D. B., and Clarke, S. D. Regulation of gene expression by dietary fat. Annu. Rev. Nutr., *19:* 63–90, 1999.

31. Mueller, E., Sarraf, P., Tontonoz, P., Evans, R. M., Martin, K. J., Zhang, M., Fletcher, C., Singer, S., and Spiegelman, B. M. Terminal differentiation of human breast cancer through PPARγ. Mol. Cell., *1:* 465–470, 1998.

32. Tontonoz, P., Singer, S., Forman, B. M., Sarraf, P., Fletcher, J. A., Fletcher, C. D., Brun, R. P., Mueller, E., Altiok, S., Oppenheim, H., Evans, R. M., and Spiegelman, B. M. Terminal differentiation of human liposarcoma cells induced by ligands for peroxisome proliferator-activated receptor γ and the retinoid X receptor. Proc. Natl. Acad. Sci. USA, *94:* 237–241, 1997.

33. Hartwell, L. H., and Weinert, T. A. Checkpoints: controls that ensure the order of cell cycle events. Science (Washington DC), *246:* 629–634, 1989.

34. Cao, Z., Umek, R. M., and McKnight, S. L. Regulated expression of three C/EBP isoforms during adipose conversion of 3T3–L1 cells. Genes Dev., *5:* 1538–1552, 1991.

35. Umek, R. J., Friedman, A. D., and McKnight, S. L. CCAAT-enhancer binding protein: a component of a differentiation switch. Science (Washington DC), *289:* 288–292, 1991.

36. Christy, R. J., Faestner, K. H., Geiman, D. E., and McKnight, M. D. CCAAT/enhancer binding protein gene promoter: binding of nuclear factors during differentiation of 3T3–L1 preadipocytes. Proc. Natl. Acad. Sci. USA, *88:* 2593–2597, 1991.

37. Wu, Z., Xie, Y., Bucher, N. L. R., and Farmer, S. R. Conditional ectopic expression of C/EBPβ in NIH-3T3 cells induces PPARγ and stimulates adipogenesis. Genes Dev., *9:* 2350–2363, 1995.

38. Gimble, J. M., Robinson, C. E., Wu, X., Kelly, K. A., Rodriguez, B. R., Kliewer, S. A., Lehmann, J. M., and Morris, D. C. Peroxisome proliferator-activated receptor-γ activation by thiazolidinediones induces adipogenesis in bone marrow stromal cells. Mol. Pharmacol., *50:* 1087–1094, 1996.

39. Hallakou, S., Doare, L., Foufelle, F., Kergoat, M., Guave-Millo, M., Berthault, M. F., Dugail, I., Morin, J., Auwerx, J., and Ferre, P. Pioglitazone induces *in vivo* adipocyte differentiation in the obese Zucker fa/fa rat. Diabetes, *46:* 1393–1399, 1997.

40. Arends, M. J., Morris, R. G., and Wyllie, A. H. Apoptosis: the role of the endonuclease. Am. J. Pathol., *136:* 593–608, 1990.

41. Kaufmann, S. H., Desnoyers, S., Ottaviano, Y., Davidson, N. E., and Poirier, G. G. Specific cleavage of poly (ADP-ribose) polymerase: an early marker of chemotherapy-induced apoptosis. Cancer Res., *53:* 3976–3985, 1993.

42. Costa, A. K., Schieble, T. M., Heffel, D. F., and Trudell, J. R. Toxicity of calcium ionophore A23187 in monolayers of hypoxic hepatocytes. Toxicol. Appl. Pharmacol., *87:* 43–47, 1987.

43. Matsubara, K., Kubota, M., Adachi, S., Kuwakado, K., Hirota, H., Wakazono, Y., Akiyama, Y., and Mikawa, H. Different mode of cell death induced by calcium ionophore in human leukemia cell lines: possible role of constitutive endonuclease. Exp. Cell Res., *210:* 19–25, 1994.

44. Reers, M., Smith, T. W., and Chen, L. B. J-aggregate formation of a carbocyanine as a quantitative fluorescent indicator of membrane potential. Biochemistry, *30:* 4480–4486, 1991.

45. Smiley, S. T., Reers, M., Mottola-Hartson, C., Lin, M., Chen, A., Smith, T. W., Steele, G. D., Jr., and Chen, L. Intracellular heterogeneity in mitochondrial membrane potentials revealed by a J-aggregate-forming lipophilic cation JC-1. Proc. Natl. Acad. Sci. USA, *88:* 3671–3675, 1991.

46. Mancini, M., Anderson, B. O., Caldwell, E., Sedghinasab, M., Paty, P. B., and Hockenbery, D. M. Mitochondrial proliferation and paradoxical membrane depolarization during terminal differentiation and apoptosis in a human colon carcinoma cell line. J. Cell Biol., *138:* 449–469, 1997.

47. Butler, R., and Young, C. Y-F. Keystone Symposia, February 21–26, 1998. Breast and Prostate Cancer, Abstract No. 204, 1998.

48. Werman, A., Hollenberg, A., Solanes, G., Bjørbæk, C., Vidal-Puig, A. J., and Flier, J. S. Ligand-independent activation domain in the N-terminus of peroxisome proliferator-activated receptor γ (PPARγ). J. Biol. Chem., *272:* 20230–20235, 1997.

49. Kubota, T., Koshizuka, K., Williamson, E. A., Asou, H., Said, J. W., Holden, S., Miyoshi, I., and Koeffler, H. P. Ligand for peroxisome proliferator-activated receptor γ (troglitazone) has potent antitumor effects

against human prostate cancer both *in vitro* and *in vivo*. Cancer Res., *58:* 3344–3352, 1998.

50. Carpenter, M., Robinson, R., and Thuy, L. Prostaglandin metabolism by human testis. Lipids, *13:* 308–311, 1978.

51. Conte, D., Laguzzi, G., Boniforti, L., Cantafora, A., Di Silverio, F., Latino, C., Lalloui, G., Mesolella, V., and Isidori, A. Prostaglandin content and metabolic activity of the human prostate. *In:* A. Crastes de Paulet, H. Thalero-Dao, and F. Dray (eds.), Prostaglandins and Reproductive Physiology, Vol. 89. Paris: INSERM, 1980.

52. Benvold, E., Svanborg, K., Bygdeman, M., and Norén, S. On the origin of prostaglandins in human seminal fluid. Int. J. Androl., *8:* 37–43, 1995.

53. Tokugawa, Y., Kunishige, I., Kubota, Y., Shimoya, K., Nobunaga, T., Kimura, T., Saji, F., Murata, Y., Eguchi, N., Oda, H., Urade, Y., and Hayaishi, O. Lipocalin-type prostaglandin D synthase in human male reproductive organs and seminal plasma. Biol. Reprod., *58:* 600–607, 1998.

54. Altiok, S.,. Xu, M., and Spiegelman, B. M. PPARγ induces cell cycle withdrawal: inhibition of E2F/DP DNA-binding activity via down-regulation of PP2A. Genes Dev., *11:* 1987–1998, 1997.

55. Elstner, E., Müller, C., Koshijuka, K., Williamson, E. A., Park, D., Asou, H., Shintaku, P., Said, J. W., Heber, D., and Koeffler, H. P. Ligands for peroxisome proliferator-activated receptor γ and retinoic acid receptor inhibit growth and induce apoptosis of human breast cancer cells *in vitro* and in BNX mice. Proc. Natl. Acad. Sci. USA, *95:* 8806–8811, 1998.

56. Kim, I. K., Lee, J. H., Sohn, H. W., Kim, H. S., and Kim, S. H. Prostaglandin A_2 and Δ^{12}-prostaglandin J_2 induce apoptosis in L1210 cells. FEBS Lett., *321:* 209–214, 1993.

57. Fukushima, M., Sasaki, H., and Fukushima, S. Prostaglandin J2 and related compounds. Mode of action in G1 arrest and preclinical results. Ann. NY Acad. Sci., *744:* 161–165, 1994.

58. Clarke, P. G. H. Developmental cell death: morphological diversity and multiple mechanisms. Anat. Embryol., *181:* 195–213, 1990.

59. Hourdry, J. Cytological and cytochemical changes in the intestinal epithelium during anuran metamorphosis. Int. Rev. Cytol. Suppl., *5:* 337–385, 1977.

60. Hornung, J. P., Koppel, H., and Clarke, P. G. H. Endocytosis and autophagy in dying neurons: an ultrastructural study in chick embryos. J. Comp. Neurol., *283:* 425–437, 1989.

61. Peluso, J. J., England-Charlesworth, C., Bolender, D. L., and Steger, R. W. Ultrastructural alterations associated with the initiation of follicular atresia. Cell Tissue Res., *211:* 105–115, 1980.

62. Clarke, P. G. H. Labelling of dying neurons by peroxidase injected intravascularly in chick embryos. Neurosci. Lett., *30:* 223–228, 1982.

63. Clarke, P. G. H. Identical populations of phagocytes and dying neurons revealed by intravascularly injected horseradish peroxidase, and by endogenous glutaraldehyde-resistant acid phosphatase, in the brains of chick embryos. Histochem. J., *16:* 955–969, 1984.

64. Clarke, P. G. H., and Hornung, J. P. Changes in the nuclei of dying neurons as studied with thymidine autoradiography. J. Comp. Neurol., *283:* 438–449, 1989.

65. Tamm, I., Kikuchi, T., and Zychkinsky, A. Acidic and basic fibroblast growth factors are survival factors with distinctive activity in quiescent BALB/c3T3 murine fibroblasts. Proc. Natl. Acad. Sci. USA, *88:* 3372–3376, 1991.

66. Mosser, D. D., and Martin, L. H. Induced thermotolerance to apoptosis in human T lymphocyte cell line. J. Cell Physiol., *151:* 561–570, 1992.

67. Gordon, S. A., Hoffman, R. A., Simmons, R. L., and Ford, H. R. Induction of heat shock protein 70 protects thymocytes against radiation-induced apoptosis. Arch. Surg., *132:* 1277–1282, 1997.

68. Samali, A., and Cotter, T. Heat shock proteins increase resistance to apoptosis. Exp. Cell Res., *223:* 163–170, 1996.

69. Mailhos, C., Howard, M. K., and Latchman, D. S. Heat shock protects neuronal cells from programmed cell death by apoptosis. Neuroscience, *55:* 621–627, 1993.

70. Green, D. R., and Reed, J. C. Mitochondria and apoptosis. Science (Washington DC), *28 1:* 1309–1312, 1998.

71. Susin, S. A., Zamzami, N., and Kroemer, G. Mitochondria as regulators of apoptosis: doubt no more. Biochim. Biophys. Acta, *1366:* 151–165, 1998.

72. Fleury, C., Neverova, M., Collins, S., Raimbault, S., Champigny, O., Levi-Meyrueis, C., Bouillard, F., Seldin, M. F., Surwit, R. S., Ricquier, D., and Warden, C. H. Uncoupling protein-2: a novel gene linked to obesity and hyperinsulinemia. Nat. Genet., *15:* 269–272, 1997.

73. Yaffe, M. P. The machinery of mitochondrial inheritance and behavior. Science (Washington DC), *283:* 1493–1497, 1999.

74. Heggeness, M. H., Simon, M., and Singer, S. J. Association of mitochondria with microtubules in cultured cells. Proc. Natl. Acad. Sci. USA, *75:* 3863–3866, 1978.

75. Ball, E. H., and Singer, S. J. Mitochondria are associated with microtubules and not with intermediate filaments in cultured fibroblasts. Proc. Natl. Acad. Sci. USA, *79:* 123–126, 1982.

76. Vale, R. D., and Fletterick, R. J. The design plan of kinesin motors. Annu. Rev. Cell Dev. Biol., *13:* 745–777, 1997.

77. Tanaka, Y., Kanai, Y., Okada, Y., Nonaka, S., Takeda, S., Harada, A., and Hirokawa, N. Targeted disruption of mouse conventional kinesin heavy chain, *kif5B*, results in abnormal perinuclear clustering of mitochondria. Cell, *93:* 1147–1158, 1998.

78. De Vos, K., Goossens, V., Boone, E., Vercammen, D., Vancompernolle, K., Vandenabeele, P., Haegeman, G., Fiers, W., and Grooten, J. The 55-kDa tumor necrosis factor receptor induces clustering of mitochondria through its membrane-proximal region. J. Biol. Chem., *273:* 9673–9680, 1998.

79. Camp, H. S., Whitton, A. L., and Tafuri, S. R. PPARγ activators down-regulate the expression of PPARγ in 3T3-L1 adipocytes. FEBS Lett., *186:* 186–190, 1999.

80. Cory, A. H., Owen, T. C., Barltrop, J. A., and Cory, J. G. Use of an aqueous soluble tetrazolium/formazan assay for cell growth assays in culture. Cancer Commun., *3:* 207–212, 1991.

81. Riss, T. L., and Moravec, R. A. Comparison of MTT, XTT and a novel tetrazolium compound MTS for *in vitro* proliferation and chemosensitivity assays. Mol. Biol. Cell, *3* (Suppl.)*:* 184a, 1992.

82. Porstmann, T., Temyck, T., and Avrameas, S. Quantitation of 5-bromo-2-deoxyuridine incorporation into DNA: an enzyme immunoassay for the assessment of the lymphoid cell proliferation response. J. Immunol. Methods, *82:* 169–179, 1985.

83. Chomczynski, P., and Sacchi, N. Single-step method of RNA isolation by acid guanidinium thiocyanate-phenol-chloroform extraction. Anal. Biochem., *162:* 156–159, 1987.

84. Esquenet, M., Swinnen, J. V., Van Veldhoven, P. P., Denef, C., Heyns, W., and Verhoeven, G. Retinoids stimulate lipid synthesis and accumulation in LNCaP prostatic adenocarcinoma cells. Mol. Cell. Endocrinol., *136:* 37–46, 1997.

85. Oberhammer, F. A., Pavelka, M., Sharma, S., Tiefenbacher, R., Purchio, A. F., Busch, W., and Schulte-Hermann, R. Induction of apoptosis in cultured hepatocytes and in regressing liver by transforming growth factor β-1. Proc. Natl. Acad. Sci. USA, *89:* 5402–5412, 1992.

86. Gunji, H., Karbanda, S., and Kufe, D. Induction of internucleosomal DNA fragmentation in human myeloid leukemia cells by 1-β-D-arabinofuranosylcytosine. Cancer Res., *51:* 741–743, 1991.

87. Shah, G. M., Kaufmann, S. H., and Poirier, G. G. Detection of poly-(ADP-ribose) polymerase and its apoptosis-specific fragment by a non-isotopic activity–Western blot technique. Anal. Biochem., *232:* 251–254, 1995.

88. Zhu, H., Fearnhead, H. O., and Cohen, G. M. An ICE-like protease is a common mediator of apoptosis induced by diverse stimuli in human monocyte THP.1 cells. FEBS Lett., *374:* 303–308, 1995.

89. McDowell, E. M., and Trump, B. F. Histologic fixatives suitable for diagnostic light and electron microscopy. Arch. Pathol. Lab. Med., *100:* 405–414, 1976.

90. Spurr, A. R. A low-viscosity epoxy resin embedding medium for electron microscopy. J. Ultrastruct. Res., *26:* 31–43, 1969

[CANCER RESEARCH 60, 4714–4718, September 1, 2000]

Advances in Brief

Tumor Prevention and Antitumor Immunity with Heat Shock Protein 70 Induced by 15-Deoxy-$\Delta^{12,14}$-prostaglandin J_2 in Transgenic Adenocarcinoma of Mouse Prostate Cells[1]

Donkena Krishna Vanaja, Michael E. Grossmann, Esteban Celis, and Charles Y. F. Young[2]

Departments of Urology [D. K. V., C. Y. F. Y.] and Immunology [M. E. G., E. C.], Mayo Clinic/Foundation, Rochester, Minnesota 55905

Abstract

The biological modifier Δ^{12}-prostaglandin J_2 and related prostaglandins have been reported to have significant growth-inhibitory activity with induction of heat shock proteins (Hsps). Tumor-derived Hsps have been shown previously to elicit specific immunity to tumors from which they are isolated. In this study, 15-deoxy-$\Delta^{12,14}$-prostaglandin J_2 (15d-PGJ_2)-induced Hsp70 was purified from transgenic adenocarcinoma mouse prostate cells (TRAMP-C2). It was then tested for its ability to activate specific CTLs and induce protective immunity against prostate cancer in C57BL/6 mice. Treatment of cells with 8.0 μM 15d-PGJ_2 for 24 h caused significant induction of Hsp70 expression. The yield of Hsp70 purified from 15d-PGJ_2-treated cells was 4–5-fold higher when compared with untreated TRAMP-C2 cells. Vaccination of mice with Hsps isolated from TRAMP-C2 cells elicited tumor-specific CTLs and prevented the growth of TRAMP-C2 tumors. These results indicate that the induced heat shock proteins may have promising applications for antitumor, T-cell immunotherapy. In particular, these findings have important implications for the development of novel anticancer therapies aimed at promoting an immune response to prostate tumors.

Introduction

Prostate cancer in its early stages is amenable to surgery, radiation treatment, and hormone therapy. The major concern is that the prognosis for late-stage metastatic prostate cancer is poor. Manipulation of the immune system appears to be a promising means that may allow elimination of metastatic cells. However, most human cancer cells are not sufficiently immunogenic to trigger an immune response *in vivo* (1–3). One possible reason for this lack of tumor cell immunogenicity is that most tumor antigens are either masked or inaccessible. One of the most effective ways to stimulate antitumor immunity has been to promote cross-priming of CTLs by host professional antigen-presenting cells (4, 5). Cross presentation is thought to occur when antigen-presenting cells take up Hsps[3] (6) and may represent a mechanism for inducing immunotherapy for prostate cancer.

The antiproliferative activity of 15d-PGJ_2 causes nonapoptotic cell death in prostate tumor cells (7). The growth-inhibitory effect of Δ^{12}-PGJ_2 on tumor cells involves the induction of Hsp70 synthesis (8). Hsp overexpression leads to an increased chaperoning of antigenic peptides into a particular subset of macrophages or other antigen-presenting cells, leading to their efficient presentation via class I or class II pathways (9, 10). Heat shock proteins activate the resting antigen-presenting cells to take up and process the tumor antigens and up-regulate the expression of costimulatory molecules necessary for T-cell activation (6). There is now comprehensive experimental evidence that the antigenicity of tumor-derived Hsp70 and gp96 preparations results from diverse arrays of endogenous peptide antigens complexed with the Hsps (11). Therefore, Hsps isolated from a patient's tumor represent a customized, patient-specific, pan-valent vaccine. This is because the Hsps chaperone an entire array of antigenic peptides generated by a tumor, instead of one or a few selected antigenic epitopes (12).

Several animal tumor models have examined the role of Hsps in antitumor responses. Vaccination of mice with Hsp preparations derived from autologous tumor cells have been shown to cause resistance to a subsequent challenge with live cancer cells in Zajdela ascitic hepatoma, in Meth A fibrosarcoma, and in B16 melanoma cells (13–15). This phenomenon has been shown with three major Hsps, gp96, Hsp90, and Hsp70. When the relative immunogenicities of the Hsps are compared in the Meth A sarcoma, the immunogenicity of Hsp90 was ~10% that of gp96 or Hsp70 (16). In the poorly immunogenic UV-induced mouse carcinomas, vaccination with gp96 preparation has been shown to elicit CTL and memory T-cell responses in addition to tumor prevention (17). These results illustrate that different Hsps may have different antigenic responses in various tumors.

Recent studies in the Dunning prostate cancer rat model showed tumor preventive response by vaccination with gp96, with delay in the development of tumor (18). However, previous work has not investigated the role of Hsps in the ability to activate tumor-specific CTLs in antiprostate tumor therapy or the role of Hsp70 in prostate cancer immunotherapy. Expression of Hsps after 15d-PGJ_2 treatment may provide a functional signal to the immune system that could contribute to the breaking of tolerance to tumor antigens that would otherwise have remained immunologically hidden. Therefore, we studied whether 15d-PGJ_2-induced Hsp expression may have an effect on recognition of prostate tumor cells by the immune system.

In our study, TRAMP-C2 cells (transgenic adenocarcinoma mouse prostate cancer C2 cells) from the TRAMP model were used to evaluate the antitumor effect of Hsps induced by 15d-PGJ_2 in a prostate cancer model. Previously, Greenberg *et al.* (19) described a spontaneous autochthonous transgenic mouse model for prostate cancer. In this mouse model, TRAMP mice, which are transgenic for the SV40 large T antigen (Tag) under the control of the rat probasin regulatory elements, express Tag at puberty (6 weeks of age; Ref. 20). The probasin regulatory element is androgen regulated and prostate specific in transgenic mice (21). The development and progression of prostate cancer in the TRAMP model closely mimics the human disease. Three cell lines, TRAMP-C1, TRAMP-C2, and TRAMP-C3 were obtained from a 32-week-old TRAMP mouse prostate adenocarcinoma. C1 and C2 are transplantable in syngeneic C57BL/6 mice. It has been shown that Tag is not expressed in C1 and C2 cells *in vitro*

Received 3/23/00; accepted 7/19/00.

The costs of publication of this article were defrayed in part by the payment of page charges. This article must therefore be hereby marked *advertisement* in accordance with 18 U.S.C. Section 1734 solely to indicate this fact.

[1] This work was supported by Department of Defense Grant DAMD 17-98-1-8523 and NIH Grants CA 70892, CA 09127, and CA 82677.

[2] To whom requests for reprints should be addressed, at Departments of Urology and Biochemistry/Molecular Biology, Mayo Clinic/Foundation, Guggenheim 1742B, 200 First Street SW, Rochester, MN 55905. Phone: (507) 284-9247; Fax: (507) 284-2384; E-mail: youngc@mayo.edu.

[3] The abbreviations used are: Hsp, heat shock protein; 15d-PGJ_2, 15-deoxy-$\Delta^{12,14}$-prostaglandin J_2; PC, peptide complex; FPLC, fast protein liquid chromatography.

or *in vivo* (22). We used TRAMP-C2 cells to investigate whether 15d-PGJ_2-induced tumor-derived Hsp70 can be used as a vaccine to generate a specific antitumor immune response to prostate cancer and to protect immune-competent C57BL/6 mice from prostate tumor growth.

Materials and Methods

Mice. Male C57BL/6 mice, 6–8 weeks of age were obtained from Jackson Laboratories (Bar Harbor, ME). Animals were housed in the Mayo Animal Resources Facilities under controlled temperature, humidity, and a 12-h of light and dark cycle with food and water *ad libitum* in the virus-free mouse facility. The animals were allowed to acclimate 5 days prior to the experiment.

Tumor Cell Lines. TRAMP-C2 cell lines were cultured in DMEM supplemented with 5% Nu-serum IV, 5% FBS, 100 units/ml penicillin, 100 units/ml streptomycin, and 5 μg/ml insulin. Murine EL4 lymphoma cell line were maintained in Iscove's modified medium with 5% FCS, 4 μl/l β-mercaptoethanol, and 10 μg/ml gentamicin.

Treatment of Cell Lines with 15d-PGJ_2. 15d-PGJ_2 was obtained from Cayman Chemical Company as a solution in methyl acetate. The solvent is changed to ethanol by evaporation of methyl acetate under a gentle stream of nitrogen. TRAMP-C2 and EL4 lymphoma cells were seeded in 10-cm culture dishes at 1×10^6 cells in DMEM and Iscove's media. The medium was changed to 5% charcoal stripped serum medium before 24 h of treatment. The cells were treated with varying concentrations of 15d-PGJ_2 for 24 h, washed once with PBS, harvested, and centrifuged at 1000 rpm for 5 min. Whole-cell lysates were prepared according to the protocol provided by Santa Cruz Biotechnology, Inc. with minor modification. Cells were washed with cold 1× PBS once and lysed in RIPA buffer [1 × PBS, 1% NP40 (Amaresco), 0.5% sodium deoxycholate, 0.1% SDS] (23). Protein concentration was determined by detergent compatible assay (Bio-Rad).

Antibodies. The anti-Hsp70 mouse monoclonal antibody was obtained from Dr. David Toft (Department of Biochemistry, Mayo). It recognizes both constitutive (Hsp73) and inducible (Hsp72) forms. Mouse anti-Hsp70 monoclonal antibodies SPA-810 and SPA-815 specific for inducible (Hsp72) and constitutive (Hsp73) forms, respectively, were obtained from StressGen Biotechnologies Corp. (Victoria, British Columbia, Canada). β-Tubulin mouse monoclonal antibody was obtained from Sigma Chemical Co. (St. Louis, MO).

Western Blot Analysis. The expression of Hsp70 in cells treated with 15d-PGJ_2 for 24 h was examined by Western blot analysis. Aliquots of the cell lysates (25 μg) or purified Hsp (1.0 μg) were resolved on 10% SDS polyacrylamide gels and transferred to nitrocellulose membrane. The membranes were blocked in 5% nonfat dry milk in TBST [20 mM Tris-HCl (pH 8.0), 137 mM NaCl, and 0.1% Tween 20] at room temperature for 1 h. Blots were incubated with Hsp70 antibody (1:5000 dilution), inducible Hsp70 antibody (1:1000), constitutive Hsp70 antibody (1:1000), or β-tubulin antibody (1:10,000) for 1 h at room temperature. Blots were washed three times with TBST and then incubated for 1 h with 1:10,000 diluted horseradish peroxidase-conjugated antimouse IgG antibody (Amersham Life Science, Arlington Heights, IL), and the proteins were detected using an enhanced chemiluminescence Western blotting analysis system (Amersham Life Science). β-Tubulin was used as the control of protein loading and transfer efficiency.

Purification of Hsp70 PCs from TRAMP-C2 and EL4 Cell Lines. Cells were seeded in T-175 cm^2 culture flasks at 4×10^6 cells and were treated with 8 μM 15d-PGJ_2 for 24 h. The cells were collected by centrifugation at 1000 rpm for 10 min. The pellet was washed with PBS and homogenized in hypotonic buffer (10 mM $NaHCO_3$ 0.5 mM pefabloc, pH 7.1), and the Hsp70 PC was isolated according to the method of Peng *et al.* (24), using ADP agarose column (Sigma) and further purified by FPLC system (Mono Q; Pharmacia Biotech). We used pefabloc SC instead of phenylmethylsulfonyl fluoride as protease inhibitor. Proteins were quantified by Bradford assay, and BSA was used as standard (Sigma).

Prophylactic Assay. Male mice, 6–8 weeks of age, were divided randomly into three groups of six animals each. Group I received 200 μl of PBS, group II received Hsp70 PCs purified from TRAMP-C2 cells, and group III received Hsp70 PCs purified from EL4 cells. Hsps were injected s.c. under the nape of the neck, in 200 μl of PBS, twice a week for 2 weeks. The animals were challenged with 3×10^6 live cancer cells (isolated on the same day) s.c. on the right flank, 10 days after the final immunization, and the kinetics of tumor growth was monitored.

Generation of CTL Effector Population. Mice were immunized as described in prophylactic assay. Ten days after the final immunization, the mice were sacrificed, spleens from mice in the same treatment group (four mice/group) were harvested, and the unfractionated splenocytes were restimulated *in vitro* with corresponding TRAMP-C2 and EL4 Hsps. The cells were cultured in 24-well plates for 6 days at a concentration of 3×10^6 cells in 1.0 ml of Iscove's medium with the addition of recombinant mouse IL-2 (50 units/ml) after 24 h of culture. Cytolytic activity was assayed after 6 days of incubation.

CTL Assay. Target cells TRAMP-C2 and EL4 were cultured in flasks with 100 units/ml IFN-γ before 72 h of CTL assay. The cells were collected by trypsinization and labeled with 300 μCi of chromium chloride (^{51}Cr) for 90 min. Effector cells were plated in 96-well plates at various E:T cell ratios in triplicates. The total reaction volume was kept at 200 μl/well. After 4 h of incubation of effector and target cells at 37°C/5% CO_2, 30 μl of cell free supernatant were collected from each well and counted in the Top Count NXT (Packard) counter. The amount of ^{51}Cr spontaneously released was obtained by incubating target cells in medium alone. The total amount of ^{51}Cr incorporated was determined by adding 2% Triton X-100 in PBS to the target cells, and the percentage of specific lysis was calculated as follows: % lysis = [(sample cpm − spontaneous cpm)/(total cpm − spontaneous cpm)] × 100.

Results

Induction of Hsps. To investigate the effect of 15d-PGJ_2 on the expression of Hsps, TRAMP-C2 cells were incubated with various concentrations of 15d-PGJ_2 (2.5–15 μM) for 24 h. The cells were harvested, and whole-cell extracts were run on a gel and then immunoblotted with Hsp70 antibody. Fig. 1*A* shows dose-dependent induction of Hsp70 protein with 15d-PGJ_2 concentrations ranging from 2.5 to 10 μM. Using Hsp70 antibody which recognizes both inducible and constitutive forms, maximum induction of Hsp70 was seen with 10 μM 15d-PGJ_2. Hsp70 in EL4 cells was also induced by 8.0 μM 15d-PGJ_2 when compared with the untreated group (Fig. 1*B*).

Purification of Hsp70 PCs. To isolate the Hsp70 PCs, the 15d-PGJ_2-treated cell lysates were purified using an ADP-agarose column, followed by ion-exchange chromatography (Mono Q FPLC system). Next, the fractions were resolved by SDS polyacrylamide gels. Whole-cell lysates and the purified fractions from the mono Q column were immunoblotted with Hsp70 antibodies specific for the inducible and constitutive forms (Fig. 1*C*). Densitometry of the purified fractions revealed that 92% of the Hsp70 from TRAMP-C2 cells is the inducible form and 8% is the constitutive form. Purified fractions from both TRAMP-C2 and EL4 cells were stained with silver nitrate. The staining shows a single band of Hsp70 on the gel from both EL4 and TRAMP-C2 cells (Fig. 1*D*). This reveals homogeneity of preparation with little or no contamination from other proteins. We also purified Hsps from TRAMP-C2 cells without 15d-PGJ_2 treatment (data not shown). The amount of the purified product of Hsp70 with 15d-PGJ_2 treatment was 4–5-fold higher as compared with untreated cells.

Generation of Tumor-specific CTL Response by Vaccination with Hsp PCs. We evaluated the ability of 15-d PGJ_2-induced Hsps to elicit a CTL response against TRAMP-C2 cells. As expected, mice treated with PBS had a low level of CTL activity against either TRAMP-C2 or EL4 targets (Fig. 2). Mice immunized with Hsps isolated from TRAMP-C2 cells developed high levels of CTL activity against TRAMP-C2 targets but not EL4 targets. Mice vaccinated with EL4 Hsps developed relatively low CTL activity against TRAMP-C2 cells or the lymphoma cells. These results indicate that the vaccination of mice with syngeneic C2 tumor-derived Hsps elicited a tumor-specific CTL response against TRAMP-C2 prostate tumor cells.

Antitumor Protection with Hsp70 PCs. To determine whether Hsp70 vaccination protects against a lethal challenge of TRAMP-C2

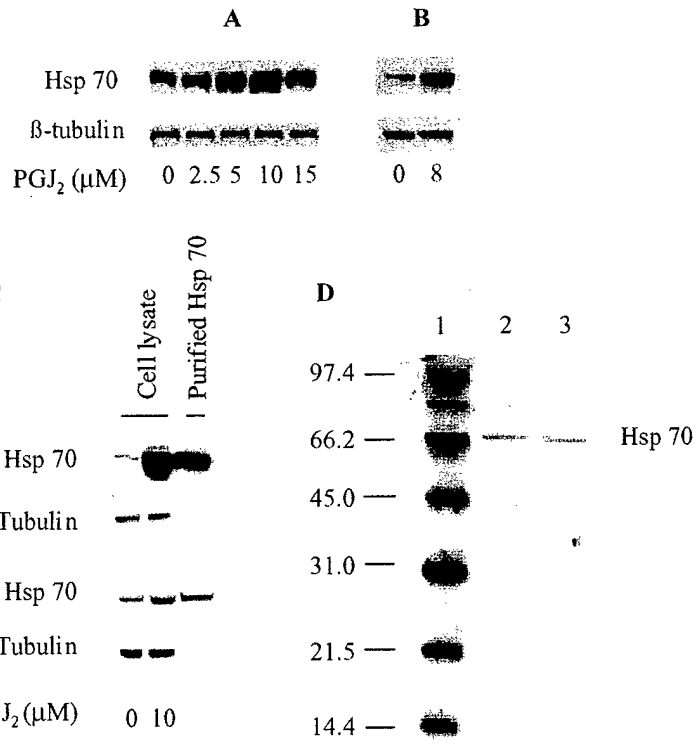

Fig. 1. *A*, 15d-PGJ_2-induced expression of Hsp70 in TRAMP-C2 cells. TRAMP-C2 cells were treated with various concentrations of 15d-PGJ_2 for 24 h and immunoblot analysis with Hsp70 monoclonal antibody recognizing both the constitutive and inducible forms. *B*, induction of Hsp70 expression in EL-4 cells with 8 μM 15d-PGJ_2. *C*, TRAMP-C2 cells treated with 10 μM 15d-PGJ_2, the whole-cell lysate, and the purified fraction of Hsp70 from the mono Q column were immunoblotted with mouse Hsp70 antibodies specific for the inducible form (Hsp72) and constitutive form (Hsp73). *D*, purified fractions of the Hsp70 from the TRAMP-C2 cells were resolved by SDA-PAGE and stained with silver nitrate. *Panel 1* is the low molecular weight marker, and *panels 2* and 3 are purified Hsp70 from TRAMP-C2 and EL4 cells, respectively.

tumor cells, the mice were injected with Hsps or PBS, and then the C2 cells were observed for tumor growth over a 9-week period. Mice pretreated with PBS and EL4 Hsps developed palpable tumors by 4 weeks after tumor challenge. The tumors grew rapidly, leading to the death of the animals within 8 weeks (Fig. 3, *A* and *B*). In contrast, mice preimmunized with Hsps isolated from 15d-PGJ_2-treated TRAMP-C2 cells showed resistance to tumor challenge, and only two of the six mice developed tumors (Fig. 3*C*). The tumors in these two mice exhibited delayed kinetics and were quite small, with the average diameter of ~5.5 mm around 7 weeks after tumor challenge. Interestingly, the tumor in one of the two mice eventually disappeared (Table 1) by the eighth week. In the second mouse, the tumor grew slowly until the end of the experiment at 9 weeks.

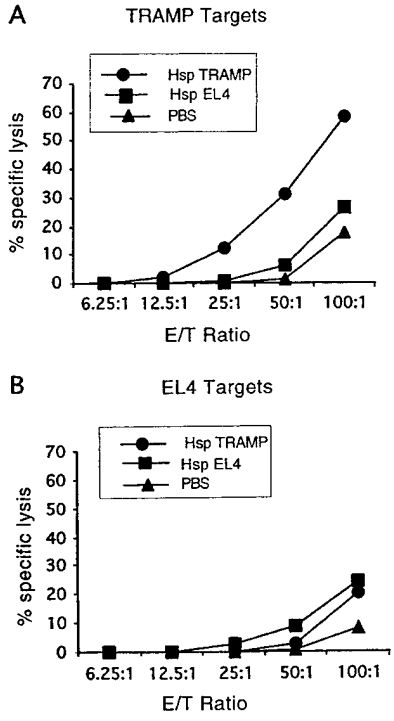

Fig. 2. Induction of CTL activity after immunization with TRAMP-C2 Hsps, EL4 Hsps, and PBS for control animals. Spleens from each group were collected 10 days after the final immunization. Pooled splenocytes from each group were restimulated *in vitro* with Hsp PCs isolated from TRAMP-C2 and EL4 cells and tested for cytolytic activity after 7 days of culture. Targets consisted of TRAMP-C2 (*A*) and EL4 (*B*) cells.

Discussion

We used TRAMP-C2 tumors in syngeneic C57BL/6 mice to evaluate the efficacy of Hsp70 vaccination in a prostate cancer model. The disease progression in the original TRAMP mice closely resembles the progression of human prostate cancer. Therefore, it is a useful model for evaluating preventive and therapeutic approaches for prostate cancer. This model should provide better correlation between animal and human antitumor results than previous models (25, 26).

We found that 15d-PGJ_2 caused nonapoptotic cell death (data not shown) with induction of Hsp70 synthesis in TRAMP-C2 cells. We have also observed 15d-PGJ_2-induced Hsp70 overexpression in other prostate cells such as TRAMP C1, LNCaP, PC3, and DU145 cells (data not shown), indicating a broad Hsp70 induction with 15d-PGJ_2. Maximum induction of Hsp70 was seen around 8–10 μM 15d-PGJ_2. The use of an ADP-affinity column allowed the isolation of immunogenic peptides associated with Hsp70, and these preparations mostly contained the inducible (Hsp72) form. It was shown previously that Hsp PCs are important for generation of antitumor immunity. Vaccination with either Hsp70 alone or the peptides alone did not elicit tumor immunity in tumor rejection models (13, 27). The antigenic epitopes bound to Hsp70 may represent a broad range of unique, shared, and nonspecific normal cellular antigens.

It was demonstrated that Hsp preparations isolated from tumor cells could be used to immunize mice against the tumors from which the

preparations were obtained (12). Immunization of mice with Hsps elicits a specific cellular immune response not against the Hsps *per se* but against antigenic peptides chaperoned by them. Results from our study demonstrate that tumor-derived TRAMP-C2 Hsp vaccination as opposed by EL4 Hsps induces a specific CTL response against the C2 cells. The appearance of CTLs specific for TRAMP-C2 cells and capable of lysing C2 cells *in vitro* correlated with the development of protective immunity against TRAMP-C2 tumors *in vivo*. Similar results were obtained when the experiment was repeated. The possible reasons for low EL4 CTL activity with EL4 cell-derived Hsps might be because the conditions for vaccinations were not optimal (*e.g.*, frequency and time interval of vaccination). Alternatively, the amount of Hsp70 PC used might be insufficient to develop a significant immune response.

A well-characterized major peptide binding Hsp70 was shown to elicit immunity to the tumors from which it was isolated but not to antigenically distinct tumors (28). The induction of Hsp72 in B16 melanoma cells significantly enhanced the immune recognition of tumor cells by increasing the levels of MHC class I antigens on their surface (29). A role of Hsp72 in the trafficking of antigenic peptides has been suggested by Srivastava *et al.* (30). They have shown that exogenous peptides administered as complexes with Hsp72 are efficiently shunted into the MHC class I presentation pathway. It was shown that Hsps localized in distinct intracellular compartments are associated with different sets of precursors for MHC class I binding, tumor antigenic peptides. The patterns of association of peptides were distinct and specific for each Hsp. In a mouse leukemia model, Hsp90 was found associated with an 8-mer epitope as well as two other precursor peptides, whereas Hsp70 was associated with only the 8-mer epitope and gp96 was associated with the 8-mer epitope and one of the 10-mer precursor peptides. The antigenic peptides associated with Hsp70 in the prostate cancer model are not yet known. However, vaccination with autologous tumor-derived Hsp PCs uses the entire antigenic repertoire of the cell, which circumvents the need to identify a large number of CTL epitopes.

Our study shows that the 15d-PGJ_2-induced Hsp72 can be used to generate a specific CTL response. The immune response elicited by Hsp72 expression was also able to protect against tumor challenge. The advantage of using Hsp PCs for vaccination is that the antitumor immune responses will be generated for the entire antigenic repertoire of the cancer cells. The observations reported in this study provide some of the important elements needed for development of Hsp peptides as the basis of a new generation of vaccines against prostate cancer.

Table 1 *Immunization of Hsp70 PCs isolated from TRAMP-C2 and EL4 cells on the tumor incidence by challenge with TRAMP-C2 cells*

The animals in the control group and EL4 Hsp group were sacrificed after 8 weeks. Tumor growth was monitored up to 9 weeks in animals that received TRAMP Hsp PCs.

	No. of weeks after challenge of 3×10^6 live TRAMP-C2 cells					
	4	5	6	7	8	9
Control (PBS)	4/6	6/6	6/6	6/6	6/6	NA[a]
Hsp70 PCs (EL 4)	5/6	6/6	6/6	6/6	6/6	NA
Hsp70 PCs (TRAMP-C2)	0/6	0/6	0/6	2/6	1/6	1/6

[a] NA, not available.

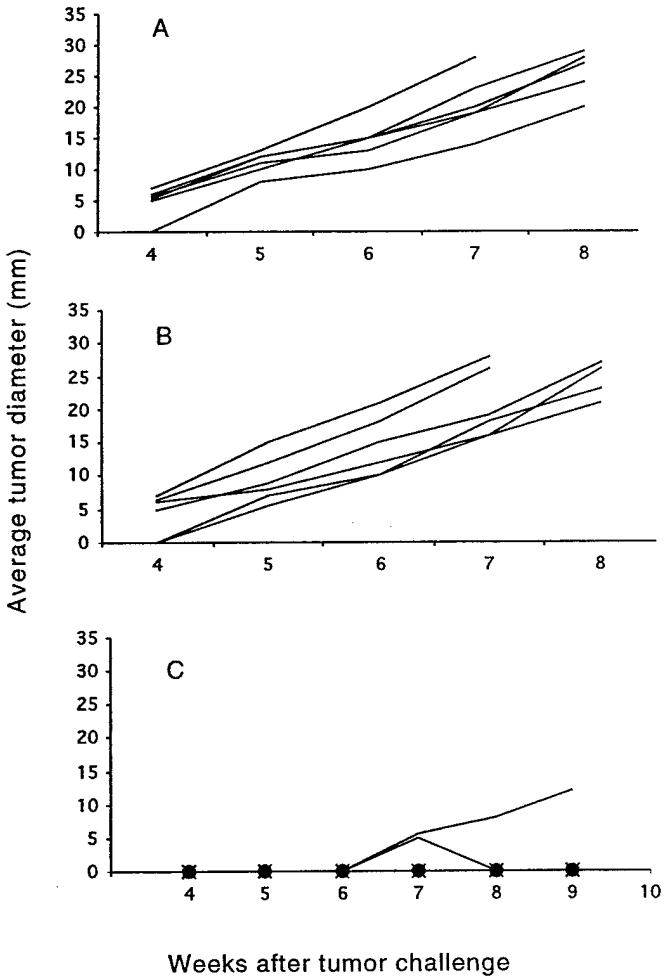

Fig. 3. Induction of antitumor protection by vaccination with Hsp70 PCs. Groups of six mice were injected with PBS for controls (*A*), Hsp PCs from EL4 cells (*B*), and Hsp PCs isolated from TRAMP-C2 cells (*C*). The animals were challenged 10 days later with s.c. injection of 3×10^6 TRAMP-C2 cells. Results depict tumor growth in individual animals over time.

Acknowledgments

We are thankful to Cris Charlesworth (protein core facility) for FPLC purification of Hsps and to Susan H. Mitchell for preparation of cell cultures.

References

1. Restifo, N. P., Esquivel, F. A., Asher, L., Stotter, H., Barth, R. J., Bennink, R. J., Mule, J. J., Yewdell, J. W., and Rosenberg, S. A. Defective presentation of endogenous antigens by a murine sarcoma. J. Immunol., *147:* 1453–1459, 1991.
2. Restifo, N. P., Esquivel, F., Kawakami, Y., *et al.* Identification of human cancers deficient in antigen processing. J. Exp. Med., *177:* 265–277, 1993.
3. Kaklamanis, L., Leek, R., Koukourakis, M., Gatter, K. C., and Harris, A. L. Loss of transporter in antigen processing 1 transport protein and major histocompatibility complex class I molecules in metastatic *versus* primary breast cancer. Cancer Res., *55:* 191–194, 1995.
4. Cayeux, S., Richter, G., Noffz, G., Dorken, B., and Blankenstein, T. Influence of gene modified (IL-7, IL-4 and B7) tumor cell vaccines on tumor antigen presentation. J. Immunol., *158:* 2834–2841, 1997.
5. Cavallo, F., *et al.* Protective and curative potential of vaccination with *interleukin-2* gene-transfected cells from a spontaneous mouse mammary adenocarcinoma. Cancer Res., *53:* 5067–5070, 1993.
6. Suto, R., and Srivastava, P. K. A mechanism for the specific immunogenicity of heat shock protein-chaperoned peptides. Science (Washington DC), *269:* 1585–1588, 1995.
7. Butler, R., Mitchell, S. H., Tindall, D. J., and Young, C. Y. F. Nonapoptotic cell death associated with S-phase arrest of prostate cancer cells via the peroxisome proliferator activated receptor γ ligand, 15-deoxy-$\Delta^{12,14}$-prostaglandin J_2. Cell Growth Differ., *11:* 49–61, 2000.
8. Ahn, S-G., Jeong, S-Y., Rhim, H., and Kim, I-K. The role of c-Myc and heat shock protein 70 in human hepatocarcinoma Hep3B cells during apoptosis induced by prostaglandin A_2/Δ^{12}- prostaglandin J_2. Biochem. Biophys. Acta, *1448:* 115–125, 1998.
9. Udono, H., Levey, D. L., and Srivastava, P. K. Cellular requirement for tumor-specific immunity elicited by heat shock proteins: tumor rejection antigen gp96 primes $CD8^+$ T cells *in vivo*. Proc. Natl. Acad. Sci. USA, *91:* 3077–3081, 1994.
10. Li, Z. Priming of T cells by heat shock protein-peptide complexes as the basis of tumor vaccines. Semin. Immunol., *9:* 315–322, 1997.
11. Srivastava, P. K., Menoret, A., Basu, S., Binder, R. J., and McQuade, K. L. Heat shock proteins come of age: primitive functions acquire new roles in an adaptive world. Immunity, *8:* 657–665, 1998.

12. Wang, X. Y., Kaneko, Y., Repasky, E., and Subjeck, J. R. Heat shock proteins and cancer immunotherapy. Immunol. Investig., *29:* 131–137, 2000.
13. Srivastava, P. K., and Das, M. R. Serologically unique surface antigen of a rat hepatoma is also its tumor-associated transplantation antigen. Int. J. Cancer, *33:* 417–422, 1984.
14. Srivastava, P. K., Deleo, A. B., and Old, L. J. Tumor rejection antigens of chemically induced sarcomas of inbred mice. Proc. Natl. Acad. Sci. USA, *83:* 3407–3411, 1986.
15. Tamura, Y., Peng, P., Kang, L., Daou, M., and Srivastava, P. K. Immunotherapy of tumors with autologous tumor-derived heat shock protein preparations. Science (Washington DC), *278:* 117–120, 1997.
16. Udono, H., and Srivastava, P. K. Comparison of tumor-specific immunogenicities of stress-induced proteins gp96, hsp90, and hsp70. J. Immunol., *152:* 5398–5403, 1994.
17. Blachere, N. E., Li, Z., Chandawarkar, R. Y., Suto, R. Jaikaria, N. S., Basu, S., Udono, H., and Srivastava, P. K. Heat shock protein-peptide complexes, reconstituted *in vitro* elicit peptide-specific cytotoxic T lymphocyte response and tumor immunity. J. Exp. Med., *186:* 1315–1322, 1997.
18. Yedavelli, S. P. K., Guo, L., Daou, M. E., Srivastava, P. K., Mittelman, A., and Tiwari, R. K. Preventive and therapeutic effect of tumor derived heat shock protein, gp96, in an experimental prostate cancer model. Int. J. Mol. Med., *4:* 243–248, 1999.
19. Greenberg, N., DeMayo, F., Finegold, M., Medina, D., Tilley, W., and Aspinall, J. Prostate cancer in a transgenic mouse. Proc. Natl. Acad. Sci. USA, *92:* 3439–3443, 1995.
20. Hsu, C. X., Ross, B. D., Chrisp, C. E., Derrow, S. Z., Charles, L. G., Pienta, K. J., Greenberg, N. M., Zeng, Z., and Sanda, M. G. Longitudinal cohort analysis of lethal prostate cancer progression in Transgenic mice. J. Urol., *160:* 1500–1505, 1998.
21. Greenberg, N. M., DeMayo, F. J., Sheppared, P. C., Barrious, R., Lebovitz, R., and Finegold, M. The rat probasin gene promoter directs hormonally and developmentally regulated expression of a heterologous gene specifically to the prostate in transgenic mice. Mol. Endocrinol., *8:* 230–239, 1994.
22. Foster, B. A., Gingrich, J. R., Kwon, E. D., Madias, C., and Greenberg, N. M. Characterization of prostatic epithelial cell lines derived from transgenic adenocarcinoma of the mouse prostate (TRAMP) model. Cancer Res., *57:* 3325–3330, 1997.
23. Zhang, S., Hsieh, M. L., Zhu, W., Klee, G. G., Tindall, D. J., and Young, C. Y. Interactive effects of triiodothyronine and androgens on prostate cell growth and gene expression. Endocrinology, *140:* 1665–1671, 1999.
24. Peng, P., Menoret, A., and Srivastava, P. K. Purification of immunogenic heat shock protein 70 peptide complexes by ADP-affinity chromatography. J. Immunol. Methods, *204:* 13–21, 1997.
25. Pollard, M. The Lobound-Wistar rat model of prostate cancer. J. Cell Biochem., *16H* (Suppl.)*:* 84, 1992.
26. Bosland, M. C. Animal models for the study of prostate carcinogenesis. J. Cell Biochem., *16H:* 89, 1992.
27. Przepiorka, D., and. Srivastava, P. K. Heat shock protein-peptide complexes as immunotherapy for human cancer. Mol. Med. Today, *Nov:* 478–484, 1998.
28. Udono, H., and Srivastava, P. K. Heat shock protein 70-associated peptides elicit specific cancer immunity. J. Exp. Med., *178:* 1391–1396, 1993.
29. Wells, A. D., Rai, S. K., Salvato, M. S., Band, H., and Malkovsky, M. Hsp72 mediated augmentation of MHC class I surface expression and endogenous antigen presentation. Int. Immunol., *10:* 609–617, 1998.
30. Ishii, T., Udono, H., Yamano, T., Ohta, H., Uenaka, A., Ono, T., Hizuta, A., Tanaka, N., Srivastava, P. K., and Nakayama, E. Isolation of MHC class I-restricted tumor antigen peptide and its precursors associated with heat shock proteins Hsp70, Hsp90, and gp96. J. Immunol., *162:* 1303–1309, 1999.